Heliyon 10 (2024) e32954

Contents lists available at ScienceDirect

Heliyon

journal homepage: www.cell.com/heliyon

Research article

Evaluation of resistance patterns and bioremoval efficiency of hydrocarbons and heavy metals by the mycobiome of petroleum refining wastewater in Jazan with assessment of molecular typing and cytotoxicity of *Scedosporium apiospermum* JAZ-20

Fuad Ameen [a,*], Mohammad J. Alsarraf [b], Tarad Abalkhail [a], Steven L. Stephenson [c]

[a] *Department of Botany& Microbiology, College of Science, King Saud University, Riyadh, 11451, Saudi Arabia*
[b] *Department of Science, College of Basic Education, the Public Authority of Applied Education and Training (PAAET), Kuwait*
[c] *Department of Biological Sciences, University of Arkansas, Fayetteville, USA*

ARTICLE INFO

Keywords:
Refinery wastewater
Bioremoval heavy metals and hydrocarbons
Antibiotic resistant
Scedosporium
Anti-proliferation
GC/MS analysis

ABSTRACT

Jazan Industrial Economic City (JIEC) is located on the Red Sea coast in the province of Jazan, southwest of Saudi Arabia anchors diverse heavy and secondary industries in the energy, water desalination, petroleum, aluminum, copper, refineries, pharmaceuticals and food manufacturing fields. These various industries generate a large quantity of industrial wastewaters containing various toxicants. The present work represents ecologically beneficial alternatives for the advancement of environmental biotechnology, which could help mitigate the adverse impacts of environmental pollution resulting from petroleum refining effluents. The mycobiome (32 fungal strains) isolated from the industrial wastewater of the refinery sector in Jazan were belonged to five fungal genera including *Fusarium*, *Verticillium*, *Purpureocillium*, *Clavispora* and *Scedosporium* with a distribution percentage of 31.25, 21.88, 15.63, 12.50 and 18.75 %, respectively.

These isolates showed multimetals tolerance and bioremoval efficiency against a large number of heavy metals (Fe^{2+}, Ni^{2+}, Cr^{6+}, Zn^{2+}, As^{3+}, Cu^{2+}, Cd^{2+}, Pb^{2+}, Ag^{+} and Hg^{2+}) along with potent bioremediation activity toward crude oil and the polycyclic aromatic hydrocarbons. Interestingly, the mycobiome resistance patterns obtained against different classes of fungal antibiotics including azole (fluconazole, itraconazole, voriconazole, posaconazole, isavuconazole and ketoconazole), echinocandin (anidulafungin, caspofungin and micafungin) and polyene (amphotericin B) drugs proved the prevalence of antibiotic resistance among the mycobiome of refinery industry in Saudi Arabia is relatively low. The fungal isolate under isolation code JAZ-20 showed the highest bioremoval efficiency against heavy metals (90.8–100.0 %), crude oil (89.50 %), naphthalene (96.7 %), phenanthrene (92.52 %), fluoranthene (100.0 %), anthracene (90.34 %), pyrene (85.60 %) and chrysene (83.4 %). It showed the highest bioremoval capacity ranging from 85.72 % to 100.0 % against numerous pollutants found in a wide array of industrial effluents, including diclofenac, ibuprofen, carbamazepine, acetaminophen, sulfamethoxazole, bisphenol, bleomycin, vincristine, dicofol, methyl parathion, atrazine, diuron, dieldrin, chlorpyrifos, profenofos and phenanthrene. The isolate JAZ-20 was chosen for molecular typing, cytotoxicity assessment, analysis of volatile compounds and optimization investigations. Based on phenotypic, biochemical and phylogenetic analysis, strain JAZ-20 identified as *Scedosporium apiospermum*

* Corresponding author.
E-mail address: fuadameen@ksu.edu.sa (F. Ameen).

https://doi.org/10.1016/j.heliyon.2024.e32954
Received 9 March 2024; Received in revised form 3 June 2024; Accepted 12 June 2024
Available online 16 June 2024

JAZ-20. This strain is newly discovered in industrial effluents in Saudi Arabia. Fungal strain JAZ-20 consistently produced various types of saturated and unsaturated fatty acids. the main fatty acids were $C_{14:0}$ (1.95 %), iso-$C_{14:0}$ (2.98 %), anteiso-$C_{14:0}$ (2.13 %), iso-$C_{15:0}$ (9.16 %), anteiso-$C_{15:0}$ (11.75 %), $C_{15:0}$ (7.42 %), $C_{15:1}$ (2.37 %), anteiso-$C_{16:0}$ (3.4 %), $C_{16:0}$ (10.3 %), iso-$C_{16:0}$ (9.5 %), $C_{17:1}$ (1.36 %), anteiso-$C_{17:1}$ (8.64 %), iso-$C_{18:0}$ (11.0 %), $C_{18:0}$ (3.63 %), anteiso-$C_{19:0}$ (3.78 %), anteiso-$C_{20:0}$ (2.0 %), iso-$C_{21:0}$ (2.44 %), $C_{23:0}$ (1.15 %), and $C_{24:0}$ (2.17 %). These fatty acids serve as natural and eco-friendly antifungal agents, promoting fungal resistance and inhibiting the production of mycotoxins in the environment. Despite being an environmental isolate, its cytotoxicity was assessed against both normal and cancerous human cell lines. The IC_{50} values of JAZ-20 extract were 8.92, 10.41, 20.0, 16.5, and 40.0 μg/mL against WI38, MRC5, MCF10A, HEK293 and HDFs normal cells and 43.26, 33.75, and 40.0 μg/mL against liver (HepG2), breast (A549) and cervix (HeLa) cancers, respectively. Based on gas chromatography-mass spectrometry (GC-MS), analysis the extract of *S. apiospermum* JAZ-20 showed 47 known volatile compounds (VOCs) for varied and significant biological activities. Enhancing the bioremoval efficiency of heavy metals from actual refining wastewater involves optimizing process parameters. The parameters optimized were the contact time, the fungal biomass dosage, pH, temperature and agitation rate.

1. Introduction

The Industrial and Economic City (JIEC) is strategically positioned along the Red Sea coastline in the Jazan Province, located in the southwest region of the Kingdom of Saudi Arabia. Notably, it hosts the port of Jazan and accommodates a multitude of industries including power generation, desalination, copper production, pharmaceuticals, and oil refineries. These industries collectively generate significant volumes of effluents containing various environmental pollutants, such as crude oil, halogenated solvents, petroleum hydrocarbons, explosives, agrochemicals, and heavy metals [1]. The harmful constituents of petroleum, including total petroleum hydrocarbons (TPH) and polycyclic aromatic hydrocarbons (PAHs), pose a significant threat to living organisms, particularly in oil-rich and developing nations [2]. Water contamination by heavy metals stands out as the most critical issues arising from industrial processes and other anthropogenic activities. Among these metals, cadmium, copper, mercury, lead, iron, manganese, aluminum, arsenic, nickel, zinc, and iron are extensively utilized across various industries and are discharged in substantial quantities through effluent disposal [1]. Furthermore, the coexistence of petroleum pollution with other pollutants, such as heavy metals and chemicals contaminants, creates synergistic effects, that escalate the overall ecological damage to ecosystems. Additionally, metals, being non-biodegradable, pose numerous threats to living organisms due to their persistence in nature, highly toxic characteristics, and prolonged half-lives once they enter the food chain. Subsequently, upon accumulation within organisms, they pose multiple risks to humans and other organisms [3].

Bioremediation, utilizing living microorganisms offers a promising strategy to alleviate the adverse impacts of organic hydrocarbons, chemicals, and heavy metals present in industrial effluents. Fungi exhibit a significant capability for the bioremoval and accumulation of heavy metals, suggesting their potential utilization as cost-effective and minimally invasive technologies for remediating sites contaminated with hydrocarbons and/or heavy metals [4]. Earlier, fungal species belonging to *Alternaria*, *Cladosporium*, *Aspergillus*, *Acremonium*, *Penicillium*, *Acarospora*, *Rhodocollybia*, *Paecilomyces*, *Cochliobolus*, *Fusarium*, *Scopulariopsis*, *Curvularia*, *Issatchenkia*, *Candida* and *Rhizopus* genera have demonstrated their capacity to adsorb heavy metals, hydrocarbons, and crude oil [5,6]. The species complex of *Scedosporium* now comprises five distinct species, among which *Scedosporium apiospermum* is globally distributed and exhibits resistance to antifungal therapies including fluconazole, amphotericin B, ketoconazole, itraconazole, terbinafine, and miconazole [7].

This study aimed to: i) isolate and characterize local fungal strains from industrial wastewater originating from the refinery industry in Jazan, Saudi Arabia; ii) screen the obtained mycobiome for its potential in mycoremediation, focusing on crude oils, polycyclic aromatic hydrocarbons, various chemical pollutants, and heavy metals; iii) evaluate the resistance patterns of the obtained fungal mycobiome against a wide range of heavy metals (Fe^{2+}, Ni^{2+}, Cr^{6+}, Zn^{2+}, As^{3+}, Cu^{2+}, Cd^{2+}, Pb^{2+}, Ag^{+} and Hg^{2+}) and antifungal (azoles, echinocandins and polyenes) drugs; iv) phenotypic, chemotypic, and genotypic characterization of the hyper active strain JAZ-20; v) assessment of the cytotoxicity of JAZ-20 extract against both human normal (WI38, MRC5, MCF10A, HEK293 and HDFs) and cancer (HepG2, A549 and HeLa) cells; and vi) identification of the chemical profile of volatile compounds produced by the highly active strain *S. apiospermum* chromatography/mass spectrometry (GC/MS) analysis. To the best of our knowledge, this study represents the first investigation into the isolation, environmental distribution, cytotoxicity, and determination of volatile metabolic profiles (GC-MS analysis) of *Scedosporium apiospermum* derived from the mycobiome of industrial wastewater in Saudi Arabia.

2. Materials and methods

2.1. Study area, samples collection and preparation of refinery wastewater for analysis

Study area is industrial area for basic and downstream industries, Jazan Industrial and Economic City (JIEC) (17° 17′ 40″ N, 42° 23′ 40″ E), province of Jazan, Saudi Arabia (Fig. 1 represent the whole map of KSA with Jizan highlighted in the southwestern; a, map of

Jazan city; b, the Jazan economic city; c, and the refinery industry in Jazan; d) [8]. A collective of 30 samples of oil refinery wastewater were collected from the drainage regions of petroleum refinery industry in sterilized polyethylene bottles and transported to the laboratory in ice tank. The collected wastewater samples were gathered, filtered and divided into two portions. The first portion was stored at 4 °C until processing during 24 h to isolate its fungal mycobiome. The second portion was preserved at −80 °C for the isolation of its fungal mycobiome but the second was kept in −80 °C until analysis both before and after treatments with the dead biomass of selected fungi under optimized and non-optimized process parameters.

2.2. Preparation the aqueous solutions of heavy metals

For comparative bioremoval activity of different fungal isolates of the mycobiome, a stock of metals solution at a concentration of 10 g of each metal under study was prepared, individually in 1 L of deionized water. The desired concentrations of multi-metals were freshly obtained by mixing successive dilution of the standard stock solution with appropriate amounts of deionized water.

2.3. Preparation of the dead fungal biomasses (adsorbent) preparation

After growing strain fungal of the mycobiome obtained in potato dextrose agar (PDA) for 10 days in the dark, spores from each fungal isolate (1×10^7 CFU/mL) were inoculated individually into 500 mL Erlenmeyer flasks containing 100 mL liquid medium (g/L; yeast extract 5, malt extract 10, peptone 5, and glucose 20 in deionized water) and incubated at 30 °C for 10 days in dark on a rotary shaker 150 rpm. The resulting biomass of each fungal isolate was filtrated through Whatman No. 1, washed many times with 0.1 M NaCl followed by deionized water to eliminate non biomass particles and then autoclaved at 121 °C for 15 min. Autoclaved biomasses were washed with 0.1 M NaCl, dried in an oven at 60 °C followed by crushing to a fine powder and kept in sterile polyethylene bottles at 4 °C until use as natural biosorbent for comparative bioremoval studies, individually.

2.4. Isolation and characterization of the fungal mycobiome of refinery wastewater

Indigenous fungal mycobiome of the refinery industrial wastewater obtained from refinery industry in Jazan, Saudi Arabia was isolated using PDA medium supplemented with petrol as sole carbon source. Refinery wastewater samples were filtered. The fungal mycobiome were isolated from filtered samples after serially diluted using the serial dilution method and then inoculated into PDA medium. The plates were incubated for 10 days at 28 °C and isolates capable of increasing in biomass with visible fungal growth criteria were transferred periodically to PDA medium. The structure of the obtained fungal mycobiome from refinery effluents was and characterized using classical macroscopic and microscopic tests as previously described [9–11].

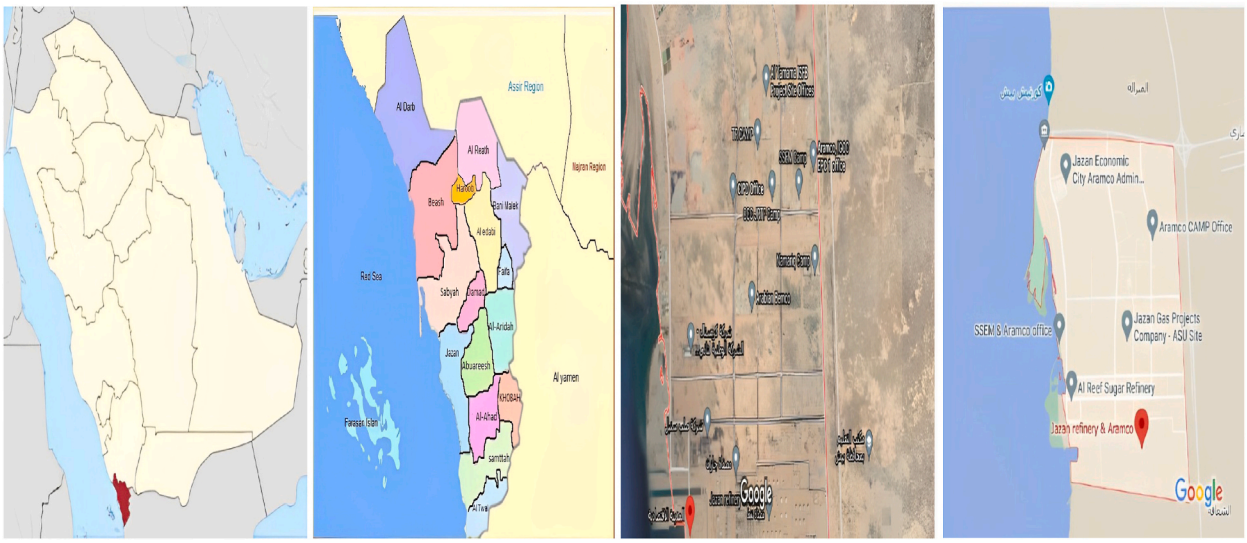

(a) (b) (c) (d)

Fig. 1. The whole map of Saudi Arabia with Jazan highlighted in the southwestern (a), the map of the Jazan city (b), the study area in Jazan economic city (c) and the refinery industry in the industrial zone of Jazan (d). (a, b, Al-Sheikh et al. [8]; c, d Google maps).

2.5. Bioremoval of crude oil, polycyclic aromatic hydrocarbons (PAHs) and other industrial pollutants from aqueous solution by the refinery wastewater mycobiome during different contact times

Experiments were conducted on the crude oil and the seven polycyclic aromatic hydrocarbons including naphthalene (NAPH), phenanthrene (PHEN), pyrene (PYR), fluoranthene (FLU), acenaphthene (ACEN), anthracene (ANTH), and chrysene (CHRY) individually from aqueous solution in batch equilibrium bioremoval experiments as described by Puszkarewicz and Kaleta [12]. Experiments were performed in flasks contains 3 g/L of crude oil or hydrocarbon, 0.5 % (w/v) of fungal biomass in 150 mL acetonitrile-water as working solution. The mixtures were agitated at 120 rpm for different contact time 6, 12, 18, 24, 36 and 48 h at 35 °C. Samples without fungal biomass were considered as controls. After each treatment, individually the concentration of the pollutant under study was determined. Bioremoval efficiencies of each pollutant by each fungus were determined following the equation: Biodegradation efficiency (%) = [weight of the polycyclic aromatic hydrocarbon (PAH) or crude oil (initial) − weight of PAH or crude oil (after treatment)]/weight of PAH or crude oil (initial) × 100].

The minimum and maximum values of bioremoval obtained among each fungal genus were stated in the Tables. Furthermore, the Bioremoval ability of the fungal isolates toward pollutants of different chemical classes, which are largely produced from pharmaceutical, petroleum, refineries, biochemical, pesticides and food industry and dumping into industrial wastewater including, were evaluated individually. These pollutants include diclofenac, ibuprofen, carbamazepine, acetaminophen, sulfamethoxazole, bisphenol, bleomycin, vincristine, dicofol, methyl parathion, atrazine, diuron, dieldrin, chlorpyrifos, profenofos and phenanthrene. The experiments were performed, individually in conical flasks each containing 3 g/L of pollutant, 250 mg/L of fungal biomass in 150 mL working solution. The mixtures were agitated at 120 rpm for 24 h at 35 °C and then the percentage of bioremoval efficiency of each compound mentioned above by tested fungal biomass was calculated following the equation: Bioremoval (%) = $(C_0–C_e)/C_0$ X 100 where C_0 is the initial concentration of chemical pollutant, and C_e is the final concentration after treatment with the tested fungus and the average percentage of bioremoval among each fungal genus was calculated and expressed. Control samples without fungal biomass were included.

2.6. Evaluation the bioremoval efficiency of heavy metals from the aqueous solution by the fungal mycobiome obtained from refinery effluents

The biosorption processes were conducted under multi-metals system in the prepared multi-metals solution. Unless stated otherwise, the biosorption experiments were performed in quick-fit flasks containing fungal biomass dosage 0.5 % (w/v) in working volume 100 mL aliquots of a mixture of Fe^{3+}, Pb^{2+}, Ni^{2+}, Cr^{6+}, Cu^{2+}, Cd^{2+}, Hg^{2+}, Ag^{+} and As^{3+} at initial concentration of 1.8 g/L (200 mg/L for each), 0.5 % of tested fungal biomass (w/v), pH 5.5, shaking rate 120 rpm at 35 °C for 60 min (contact time). After treatments, samples were digested using Anton-Paar microwave digestion method [13] and each supernatant was analyzed for residual concentration of each metal. Heavy metal solutions without biomass were assisted as control, trials were conducted in duplicate and average values were calculated. The data was recorded in percentage using the equation: Removal efficiency (RE %) = (Ci − Cf)/Ci × 100. Where R is the biosorption percentage % of the studied metal; C_i, is the initial concentration and C_f, is the residual concentration (mg/L) of the same metal under study after the biosorption process. The atomic absorption spectroscopy (AAS) was used for determining the concentration of heavy metals by the specific lamb at the specific wavelength for each metal ion.

2.7. Evaluation of IC_{50} and MICs of heavy metals against fungal mycobiome of petrol refining wastewater

Heavy metal resistance levels among soil fungi isolated from metal amended plates (100 μg/mL) were assessed by determining minimum inhibitory concentration (MIC) of individual metal against test fungi by spot plate method [14]. Briefly, different sets of SDA incorporated with varying concentrations of heavy metals, individually in a concentrations ranged from 0.10 to 6.0 g/mL was prepared as described previously [1,4]. An inoculum of examined fungal spore (10^6 CFU/mL) was spotted in duplicate on metal amended and control plates (plates containing no metal). The plates were incubated at 28 °C for seven days to be examined for the growth of fungi on the spotted area. MIC was defined as the lowest concentration of metal that inhibited the visible growth of inoculated fungi and expressed in μg/mL.

2.8. Antifungal susceptibility test

Determination of MIC for each antibiotic against each fungal isolate was determined in triplicate by micro-broth dilution method [15,16]. The tested antifungal drugs were azoles (fluconazole, itraconazole, voriconazole, posaconazole, isavuconazole and ketoconazole), echinocandins (anidulafungin, caspofungin, and micafungin) and polyenes (amphotericin B) antibiotics (Sigma, St. Louis, MO, USA). The doses of each antibiotic were prepared from stock solution (2 mg/mL) from which 30 μL was added to each well in 96 well microtiter plates; thereafter each fungal suspension (inoculum size 2.0×10^4 CFU/mL), individually was added to each well. All plates were incubated at 28 ± 2 °C for 5 days. The MIC of each antibiotic was determined as the lowest antibiotic dose in the well of the microtiter plate showed no turbidity after incubation. The MFC was determined by sub-culturing the content of each well showed no growth. MFC defined as the lowest concentration of each antibiotic resulting in the death of 99.9 % of the inoculum [16].

2.9. Characterization of the hyperactive isolate JAZ-20

For scanning electron microscopy; conidia samples from JAZ-20 were initially fixed for 1 h in 2.5 % glutaraldehyde in 0.1 M sucrose phosphate buffer (SPB) followed by three times washes with SPB at room temperature. Conidia samples were post-fixed in 1 % osmium tetroxide in SPB for 1 h, washed again, dehydrated and air-dried overnight. Conidia samples were mounted on an aluminum stub and coated with a gold film (20 nm-thickness) using a sputter coater (Ashford, UK) and the ultrastructure of conidia samples was observed in the Electron Microscope Unit, Central Lab. National research Centre, Egypt. Analysis of the fatty acid profile including saturated and non-saturated fatty acids of the hyperactive isolate JAZ-20 was done by GC/MS analysis at the GC/MS unit, Central Lab., National Research Centre, Egypt.

For DNA extraction; amplification and sequencing of the selected fungal strain JAZ-20, mycelium was harvested from seven-day-old cultures in potato dextrose broth (50 mL) and ground in liquid nitrogen with a mortar and pestle. DNA was recovered using the DNeasy Tissue Kit (Qiagen Inc.) following the manufacturer's protocol. DNA concentration was determined using spectrophotometer at 260 nm. Amplification of ribosomal DNA was performed using puReTaq™ Ready-To-Go™ beads (GE Healthcare) with the primers of ITS1 (5′-TCCGTAGGT GAACCTGCGG-3′) and ITS4 (5′-TCCTCCGCTTATTGATATGC-3′) [17]. PCR amplification performed according to previous studies [4,17–20]. PCR products tested to determine their correct length and then PCR products were purified and sequenced [18]. For phylogenetic analysis, sequence data were edited with Lasergene SeqMan (DNAStar Inc.) and compared by individual BLASTn (Basic Local Alignment Search Tool, http://www.ncbi.nlm.nih.gov) searches using NCBI (National Centre for Biotechnology Information) BLAST database for identification at the species level. Sequences were aligned using the ClustalW algorithm and phylogenetic analysis was conducted using MEGA-X by using the neighbor-joining method [21,22]. Support of internal branches was assessed using a 1000 bootstrapped data set *Petriella musispora* CBS 74569 strain was chosen as out group. The ITS region of the nuclear rDNA sequence of JAZ-20 strain has been submitted in GenBank database.

2.10. Refinery wastewater analyses

For the analyses of wastewater, 30 samples collected from different points in the oil refinery areas in Industrial Economic City, Jazan, Saudi Arabia were mixed to make a suitable representative sample and then subjected to filtration under reduced pressure, acid digestion according to APHA [13] followed by determination the initial and final concentrations of metal ions concentrations before and after treatments with JAZ-20.

2.11. Optimization of the bioremoval process parameter to enhance the remediation efficiency of heavy metals from the real refinery wastewater by the dead biomass of JAZ-20 strain

For bioremoval optimization studies, batch experiments were carried out in 250-mL Erlenmeyer flasks containing real refinery wastewater, following optimization a one-factor-at-a-time method. The influence of contact time (process time) between biomass and wastewater on metal bioremoval by isolate JAZ-20 strain was evaluated at various contact times 10, 20, 30, 60, 120 and 180 min. Moreover, the effects of the dead fungal biomass dosage (0.05, 0.1, 0.2, 0.5 and 1.0 %; w/v) were evaluated at the optimum contact time. The impact of pH by varying the initial solution pH to 2, 3, 4, 5 and 6 using dilute HCl or NaOH for adjusting pH on metal biosorption by isolate JAZ-20 was assessed. The pH values of the experiment are not set higher than 6 for avoiding any metal precipitation as hydroxide. At the optimum contact times, biomass dosage and pH value for each metal, the effect of temperature (35, 40, 45, 50 and 60 °C) and agitation rate (100, 125, 150, 200 and 250 rpm) on the bioremoval capacity of the heavy metals; Fe^{3+}, Pb^{2+}, Hg^{2+}, Ni^{2+}, Al^{3+}, Cd^{2+}, Mn^{2+}, Cr^{6+} and As^{3+} from refinery wastewater by the dead biomass of isolate JAZ-20 were evaluated. In all experiments, flasks were allowed for equilibrating on a rotating shaker and samples were collected after the appropriate period, aqueous solutions were filtered and each filtrate analyzed for residual concentration of each metal as well as its biosorption efficiency (%) to identify the most effective process parameters for achieving maximum biosorption of metal ion under evaluation.

2.12. Cultivation and extraction procedure of secondary metabolites

The fungus strain JAZ-20 was cultivated on potato dextrose broth by placing agar blocks of pure culture of actively growing culture in 1000 mL Erlenmeyer flasks containing 200 mL of the medium. The flasks were incubated at 150 rpm for 14 days at 28 ± 2 °C. To collect both extracellular and intracellular metabolites; cultured of JAZ-20 was extracted three times with ethyl acetate at room temperature (1:1). The resultant metabolites were dried in vacuum evaporator to yield the crude extract. After evaporation a brown crude extract was obtained for further processes. Extract was kept in the deep freezer at −20 °C until cytotoxicity and gas chromatography-mass spectrometry (GC-MS) analysis were performed.

2.13. Assessment of anti-proliferative activity of the selected fungal strain JAZ-20 extract

Overall the cytotoxicity of JAZ-20 extract against normal human mammary epithelial (MCF10A), normal human lung fibroblasts (WI38), normal human fetal lung fibroblast (MRC5), normal human embryonic kidney (HEK293) and dermal fibroblasts (HDFs) cell lines as well as liver cancer HepG2, cervix cancer HeLa and breast cancer A594 cells obtained from the American Type Culture Collection was determined. Cells were cultured in exponential growth in DMEM (Dulbecco's modified Eagle's medium) supplemented with 10 % heat-inactivated fetal bovine serum, 2.0 mM glutamine, 100 mg/mL streptomycin and 100 U/mL penicillin and kept at 37 °C

in a humidified atmosphere of 5 % CO_2. The effects of JAZ-20 extract on cell viability were assayed by the MTT [3-(4, 5-dimethylthiazol-2-yl)-2, 5-diphenyltetrazolium bromide] colorimetric method which measures viable cells by assessing metabolic integrity [23]. Exponentially growing cells were plated in 96-well plates and treated with increasing concentrations (0, 5, 10, 20, 30, 40, 50, 60, 70, 80, 90 and 100 μg/mL) of JAZ-20 extract after 24 h of growth. Negative controls received the same amount of DMSO. After 48 h, MTT solution was added to each well at a concentration of 0.5 mg/mL and incubated at 37 °C for 3 h. The amount of MTT-formazan product, dissolved in acidified isopropanol was estimated by measuring the absorbance at 570 nm in a microplate reader (Biorad, Model 550) and calculation of IC_{50} was done.

2.14. Gas chromatography mass spectrometry (GC-MS) analysis of the crude extract and identification of volatile bioactive compounds

Gas chromatography-mass spectrometry (GC-MS) analysis of the fungal extract JAZ-20 was made using Varian 4000 Ion trap GC/MS/MS with Fused silica 15 m × 0.2 mm ID × 1 μm of capillary column to recognize the volatile bioactive compounds (VOCs). The instrument was initially set to a temperature of 110 °C and maintained at this level for 2 min. Subsequently, the oven temperature was increased to 280 °C at a rate of 5 °C per minute. Injection port temperature was ensured as 250 °C and helium flow rate as 1 mL/min. The ionization voltage was 70eV. The samples were injected in split mode as 10:1. Mass spectral scan range was set at 45–450 (m/z). The interpretation of the mass spectrum using GC-MS-MS was performed by comparing the spectrum of unknown components in the extracts with the spectra of known components stored in the Wiley and NIST libraries of the National Institute of Standards and Technology (NIST).

2.15. Statistical analysis

The results were statistically processed by analyzes of variance (ANOVA), followed by Tukey's tests when significant effects were detected ($P \leq 0.05$). Data were expressed as means ± standard error.

Table 1
Macroscopy and microscopy characterization of the fungal mycobiome of refinery wastewater in Jazzan.

Fungal group	Phenotypic characteristics	Fungal group
JAZ-1 to JAZ-10 (n= 10, 31.25 %)	Colonies of this group JAZ-1 to JAZ-10 growing rapidly, 7.0 cm in five days, flat and spreading. Aerial mycelium fluffy to wooly and bright white in color turned to buff-brown with age with darkish blue reverse. Microscopic examination showed characteristic banana-shaped macroconidia from single, short and multiple branched conidiophores. Macroconidia on aerial conidiophores (blastoconidia) were borne singly, slightly curved with foot-cell, 3-5 septate, fusiform to curved, 20–45 × 3.0–4.5 μm. Microconidia were sparse, straight or curved, cylindrical to ellipsoid, 1–2 celled and formed from long lateral phialides, 6–14 × 2.1–4.0 μm. Chlamydospores were sparse, terminal or intercalary, hyaline, smooth to rough-walled, spherical, borne singly or in pairs on short lateral hyphal, 6.5–11.5 μm.	***Fusarium***
JAZ-11 to JAZ-17 (n= 7, 21.88 %)	Dark grey to dark pinkish grey powdery to hairy colonies with dark black margins and dark blackish brown reverse. This group was characterized by verticillate branching of hyaline conidiophores due to the branches occurs in whorls at most of their length. Conidiophores were well differentiated, erect bearing the divergent phialides, which were whorls, slender long and arranged in verticils around the conidiophore and pointy at the tips. Conidia were 3.0–12.5 μm in length, hyaline one-celled and oval to pyriform in shape, solitary or form clusters in slimy heads at the tips of the phialides (glioconidia).	***Verticillium***
JAZ-18 to JAZ-23 (n= 6, 18.75 %)	Colonies of the 6 isolates on MY agar were 50–60 mm in five days, hairy or fluffy, round to slightly oval, flat or slightly raised, spreading, smoky grey to greyish-brown being olivaceous grey with white to creamy edge and blackish to dark tan reverse. Microscopic examination showed thin and septate hyphae with large end apical. The conidiogenous cells are cylindrical, free or intercalary and have an inflated base in brush-like arrangement. Conidiophores were solitary and cylindrical with graphium morphology. Graphium were synanamorph, 133–340 μm, consist of erect, stiff bundles of terminating hyphae in a brush conidiogenous cells. The conidia were grey to brownish grey, ovoid to ellipsoidal, thick-walled with diameter of 8.22–10.1 × 3.98–5.98 μm. Subglose to globose cleistothecia were present	***Scedosporium***
JAZ-24 to JAZ-27 (n= 4, 12.50 %)	All 4 isolates showed essentially the same morphological characteristics. On Malt extract agar yeast-like colonies, convex, smooth, glabrous with entire margins were observed. They were white to creamy in color with whitish orange to creamy brown reverse were observed. In MY broth after growth for 3 days at 28 °C cells were ovoid to elongate (2–5.5 × 3.5–7 μm) and occur singly or in pairs. Multilateral budding cells, ovoid to ellipsoidal budding blastoconidia, 1.5–6.0 × 2.5–10 μm in diameter were observed. Hyphae are not produced, but pseudohyphae with blastoconidia were observed.	***Clavispora***
JAZ-28 to JAZ-32 (n= 5, 15.63 %)	After 7 days of cultivation on malt extract agar at 28 °C, growth was rapid growing reaching 40–50 mm, colonies were pale lilac to bright purple developed to a reddish-grey color, swollen round shaped, woolly to floccose with shallow radiating furrows, reverse was yellow to dim olive. Microscopic morphology showed hyaline long smooth-walled and septate hyphae with chains of conidia. Irregularly branched conidiophores rose from submerged hyphae, 400 μm–600 μm in length with smooth or rough-walled conidiophore stipes and bearing tightly clusters of typical elongated flask-shaped phialides with long narrowing neck and a broader base. Long branching chain of hyaline, ovoid or fusiform unicellular and smooth to slightly roughen walled conidia into a brush-like structure (2.3–3.5 × 2.20–2.5 μm) were observed.	***Purpureocillium***

3. Results and discussion

3.1. Characterization the mycobiome of the refinery wastewater at the Jazan Economic City

Jazan Economic City's development (Fig. 1 represent the whole map of KSA with Jizan highlighted in the southwestern; a, map of Jazan city; b, the Jazan economic city; c, and the refinery industry in Jazan; d) is based upon the philosophy of symbiotic development, incorporating co-existing uses to the benefit of each of the components and the environment [8]. Thus treatment of the industrial effluents by their adapted mycobiomes is an argent need [4]. Thirty-two isolates obtained from the mycobiome refinery wastewater were characterized into five groups each group represent one fungal genus (Table 1). The first group comprises 10 isolates under the isolation codes JAZ-1 to JAZ-10, which constituted 31.25 % of mycobiome obtained. Colonies characteristics of this group (JAZ-1 to JAZ-10) were growing rapidly to reach 7.0 cm in five days of growth on MYA medium, flat and spreading along with bright white in color turned to buff-brown and fluffy to wooly aerial mycelium with darkish blue reverse. Moreover, microscopic analysis revealed the existence of distinctive banana-shaped macroconidia from individual, shortened, and multiplies branched aerial conidiophores (blastoconidia). Macroconidia were borne singly with foot-cell, fusiform to slightly curved, 3-5 septate, 20–45 × 3.0–4.5 μm in size while microconidia were sparse, straight or curved, cylindrical to ellipsoid, 1-2-celled and formed from long lateral phialides, 4–10 × 2.0–3.9 μm. Spare hyaline, spherical, smooth to rough-walled chlamydospores borne singly or in pairs on short lateral hyphal branches or intercalary with a diameter equal to 6.5–11.5 μm were observed. Both the macroscopic appearance and microscopic characteristics of these 10 isolates from the first group strongly indicated their membership within the genus *Fusarium* (Table 1).

However, the isolates in the second group JAZ-11 to JAZ-17 (n = 7, 21.88 %) exhibited comparable traits, including a powdery to hairy texture, dark grey to dark pinkish-grey coloration with dark black margins, and a blackish to dark brown reverse. Furthermore, their microscopic examination revealed distinctive verticillate branching of hyaline conidiophores due to the branches occurring in whorls along most of their length. Conidiophores were erect, bearing divergent phialides, which were whorls, slender long and arranged in verticils around the conidiophore and pointy at the tips. The conidia ranged from 3.0 to 12.5 μm in length, appearing as hyaline, single-celled, and oval to pyriform in shape, either solitary or forming clusters in slimy heads at the tips of the phialides (glioconidia). These morphotypic features indicate that the isolates from this group are candidates for the genus *Verticillium* (Table 1). Colonies of the six isolates under isolation codes JAZ-18 to JAZ-23 (n = 6, 18.75 %) grown on MYA medium measured 50 to 60 mm in diameter after five days. They exhibited a hairy or fluffy texture and were generally round to slightly oval, with a flat or slightly raised profile. The colonies spreading and displayed a color ranging from smoky grey to greyish-brown being olivaceous grey in aged cultures, with a creamy white edge and a reverse side appearing dark brownish-black. Microscopic examination showed thin and septate hyphae with large end apical, cylindrical, free or intercalary have an inflated base in brush-like arrangement conidiogenous cells, solitary and cylindrical conidiophores with graphium morphology. Graphium were synanamorph, 133–340 μm, contain erect, rigid bundles of terminating hyphae in a brush conidiogenous cells. Grey to brownish, ovoid to ellipsoidal, thick-walled conidia with diameter of 8.22–10.1 × 3.98–5.98 μm were observed in addition to subglose to globose cleistothecia noticed at maturation. Based on these criteria, these isolates were belonging to *Scedosporium* species (Table 1).

All four isolates of the fourth group constituted 12.5 % of refinery effluents mycobiome showed essentially the same morphological characteristics. On Malt extract agar, they had creamy in color with whitish orange to creamy brown reverse yeast-like convex, smooth, glabrous with entire margins colonies. On Malt yeast extract broth, after 3 days at 28 °C cells were ovoid to elongate (2–5.5 × 3.5–7 μm) and occur singly or in pairs Hyphae are not produced, but pseudohyphae with blastoconidia were observed and multilateral budding cells, ovoid to ellipsoidal budding blastoconidia with a diameter 1.5–6.0 × 2.5–10 μm were detected. Both the macroscopic and microscopic characteristics of the cultures of these isolates were highly suggestive of *Clavispora* species (Table 1).

Finally isolates of the fifth group (JAZ-28 to JAZ-32, n = 5, 15.63 %) after 7 days of cultivation on malt extract agar at 28 °C, showed rapid growth reaching 40–50 mm and developed colonies were swollen round shaped, woolly to floccose with shallow radiating furrows and pale lilac to bright purple in color turned to reddish grey with age with yellow to dim olive reverse. Microscopic observation showed hyaline long smooth-walled and septate hyphae. Irregularly branched conidiophores rose from submerged hyphae, 400 μm–600 μm in length with smooth or rough-walled conidiophore stipes and bearing tightly clusters of typical elongated flask-shaped phialides with long narrowing neck and a broader base. Long branching chain of hyaline, ovoid or fusiform unicellular and smooth to slightly roughen walled conidia into a brush-like structure (2.3–3.5 × 2.20–2.5 μm) were observed. Both the macroscopic and microscopic morphology suggested that the five isolates assigned to the genus *Purpureocillium* (Table 1).

The fungal mycobiome in this study was characterized to the genus level using the methods outlined as described previously [9–11, 24–26]. In accordance with our results, different fungal species were isolated from industrial wastewater including *Aspergillus*, *Penicillium*, *Fusarium*, *Acremonium*, *Lecanicillium*, *Emmia*, *Curvularia* and *Mucor* species [19,20]. Notably, in this study, to the best of our knowledge, environmental isolates of *Scedosporium* species have been discovered for the first time in industrial wastewater in Saudi Arabia. *Scedosporium* species including *S. apiospermum* are emerging filamentous fungi characterized by septate hyphae and have previously been isolated in areas heavily impacted by human activity, such as public parks and industrial sites [27].

3.2. The reduction of crude oil and polycyclic aromatic hydrocarbons by the indigenous fungal strains of refinery wastewater mycobiome

Bioremediation technologies are consistently anticipated to provide an efficient, cost-effective, and environmentally friendly alternative for pollutant cleanup [28]. The bioremediation percentages of the crude oil and polycyclic aromatic hydrocarbons (PAHs), which vary in their ring structure and arrangement including phenanthrene (PHEN), fluoranthene (FLU), naphthalene (NAPH), anthracene (ANTH), chrysene (CHRY) and pyrene (PYR) were determined over a contact time ranging from 6 to 48 h. The results

indicated that the bioremoval of PAHs and crude oil by all indigenous fungal strains under study increased with the prolonged process period from 6 to 48 h (Table 2). Reduction efficiency (RE) equal to 81.14–92.11 %, 69.57–92.15 %, 80.53–90.58 %, 79.00 - 91.50 % and 93.20 - 96.70 % were occurred in the simplest PAH, naphthalene, having two aromatic rings concentration after treating with dead biomass of the isolates of *Fusarium*, *Verticillium*, *Purpureocillium*, *Clavispora* and *Scedosporium*, respectively. The capacity of fungi to degrade polycyclic aromatic hydrocarbons (PAHs) like naphthalene is of particular interest, as it was previously believed that eukaryotes lacked the ability to break down fused-ring aromatics [29]. Potent reduction ability occurred in the concentrations of the tricyclic species including phenanthrene (RE = 73.16–82.44 %, 40.53–65.15 %, 50.24–61.18 %, 36.02–51.19 % and 75.14–92.52 %), anthracene (RE = 73.32–88.21 %, 44.78–52.86 %, 61.00–76.27 %, 50.16–55.20 % and 80.25–90.34 %) and fluoranthene (RE = 71.29–80.13 %, 80.51–86.00 %, 76.29–80.43 %, 80.19–90.27 % and 98.23–100.00 %) by dead biomass of the isolates of *Fusarium*, *Verticillium*, *Purpureocillium*, *Clavispora* and *Scedosporium*, respectively. Agrawal et al. found that *G. lucidum* able to degrade 99.65 % of phenanthrene and 99.58 % of pyrene at 27 °C by producing significant amounts ($p < 0.0001$) of ligninolytic enzymes (Laccase, lignin peroxidase and manganese peroxidase) [30].

Interestingly the dead biomass of the fungal mycobiome under study showed high affinity for absorbing and then reducing the concentrations of the four-ring compounds including chrysene (RE = 50.15–60.51 %, 26.51–39.48 %, 50.18–71.13 %, 23.25–35.17 % and 70.26–83.40 %) and pyrene (RE = 50.19–67.38 %, 30.12–46.12 %, 40.80–70.11 %, 27.38–48.58 % and 69.18–85.60 %) by using the dead biomass of the isolates of *Fusarium*, *Verticillium*, *Purpureocillium*, *Clavispora* and *Scedosporium*, respectively. The PAHs under study has been listed by the United States Environmental Protection Agency (USEPA) as priority pollutants. Polycyclic aromatic hydrocarbons (PAHs) are a large group of chemicals. They represent an important concern due to their widespread distribution in the environment, their resistance to biodegradation, their potential to bioaccumulate and their harmful effects in this regard fungal strains such as *Phanerochaete chrysosporium*, *Pleurotus ostreatus* and *Bjerkandera adusta* are most commonly as a promising option and powerful choice for degradation of PAHs [31].

As a result of the ongoing increase in energy demands and advancements in oil recovery technology, the extraction, refining, and utilization of crude oil are expanding globally. Overall the biodegradation rate of crude oil ranged between 72.16 and 83.13 %, 44.55–66.25 %, 64.29–70.03 %, 26.82–45.63 % and 80.35–89.5 % by using the refinery effluents mycobiome composed of *Fusarium*, *Verticillium*, *Purpureocillium*, *Clavispora* and *Scedosporium* isolates, respectively. Because of the intricate composition of crude oil, its limited fluidity, and its biological toxicity, environmental pollution caused by petroleum has emerged as an ongoing menace to both human society and the natural environment [32]. Given its affordability, environmentally friendly nature, and capacity to completely

Table 2
Bio-remediation rate of PAHs and crude oil by different fungal genera isolated from the industrial wastewater of refinery industry in Jazzan.

Fungal group	Bio-remediation rate by different fungal genera (%) from aqueous solutions[a]							
	Contact time (h)	Crude oil	Naphthalene (NAPH)	Phenanthrene (PHEN)	Fluoranthene (FLU)	Anthracene (ANTH)	Chrysene (CHRY)	Pyrene (PYR)
***Fusarium*(n= 10, 31.25 %)**	**6**	8.50–20.17	18.90–20.43	0.00–5.18	18.00–24.15	21.74–34.88	6.02–8.92	2.50–8.14
	12	19.82–32.01	27.35–40.19	22.65–40.36	34.50–42.60	33.50–48.21	12.58–20.34	4.39–12.25
	18	30.60–41.39	38.70–59.76	36.20–58.31	40.37–50.19	41.29–60.79	19.37–31.26	10.00–20.40
	24	40.26–58.16	57.16–68.41	50.19–68.15	56.93–64.00	55.32–71.21	25.27–40.52	21.78–38.61
	36	59.84–70.37	71.90–83.52	66.11–75.21	70.00–75.42	61.50–80.79	34.17–43.24	30.85–52.13
	48	72.16–83.13	81.14–92.11	73.16–82.44	71.29–80.13	73.32–88.21	50.15–60.51	50.19–67.38
***Verticillium* (n= 7, 21.88 %)**	**6**	0.00–12.56	22.60–34.00	0.00–8.18	13.22–18.50	6.52–13.90	0.00–1.182	0.00–6.00
	12	5.18–27.39	26.71– 40.65	5.15–17.76	25.18–30.42	11.72–20.15	6.29–13.44	10.27–19.23
	18	16.40–39.19	44.50–60.83	19.14–28.01	40.51–46.30	20.18–29.74	10.71–20.50	13.01–25.19
	24	24.58–50.20	58.17–72.10	25.89–40.34	48.13 - 60.50	30.70–36.50	16.82–28.17	17.44–29.51
	36	32.15–60.05	65.22–80.40	30.21–55.43	63.20–71.16	38.15–47.90	20.27–34.93	21.92–39.62
	48	44.55–66.25	69.57 - 92.15	40.53–65.15	80.51–86.00	44.78–52.86	26.51–39.48	30.12–46.12
***Purpureocillium* (n= 5, 15.63 %)**	**6**	8.11–16.24	17.42–23.63	0.00–4.15	20.88–22.30	19.08–35.90	1.25–6.74	0.00–5.18
	12	14.92–25.33	24.18–37.90	12.11–25.13	39.35–40.61	31.33–54.33	4.30–12.00	7.15–18.50
	18	22.39–34.21	45.93–50.31	15.20–30.40	46.42–50.18	43.88–60.87	9.25–21.89	18.41–30.76
	24	38.62–49.12	57.23–69.65	24.13–36.81	59.83–64.76	53.26–60.92	16.48–31.27	29.16–40.21
	36	51.02–65.80	64.90–78.00	21.29–39.61	70.11–73.50	59.40–63.88	30.51–49.19	33.19–52.19
	48	64.29–70.03	80.53–90.58	50.24–61.18	76.29–80.43	61.00–76.27	50.18–71.13	40.80–70.11
***Clavispora* (n= 4, 12.50 %)**	**6**	0.00–5.39	11.40– 23.63	0.00–3.71	16.82–20.19	4.82– 9.50	0.00–3.21	6.17–10.02
	12	4.99–12.93	30.45–47.00	10.03–12.25	25.60–39.42	13.60–20.83	5.38–10.18	10.90–16.42
	18	9.31–20.53	41.62– 60.50	15.27–20.24	34.88–47.26	25.86–32.18	9.60–17.42	15.64–20.42
	24	18.17–39.60	53.34 - 71.12	18.90–38.23	50.73–63.40	39.80–41.16	11.14–20.51	18.37–32.34
	36	26.51–44.91	66.25 - 83.35	28.45–43.91	66.20–71.63	46.02–50.23	19.42–26.05	20.97–40.65
	48	26.82–45.63	79.00 - 91.50	36.02–51.19	80.19–90.27	50.16–55.20	23.25–35.17	27.38–48.58
***Scedosporium* (n= 6, 18.75 %)**	**6**	13.88–20.76	24.29 - 38.00	4.34–10.60	30.61–47.15	20.90–41.75	9.16–23.54	5.16–9.72
	12	27.98–39.11	40.57 - 59.80	30.00–63.14	59.30–70.86	30.16–50.86	20.00–35.48	17.83–30.63
	18	45.11–53.60	74.30 - 80.16	41.18–72.55	80.25–84.50	66.14–70.16	27.53–42.72	28.45–50.91
	24	52.32–64.35	80.00 - 87.13	60.74–81.49	85.16–90.71	70.14–81.22	40.15–56.88	40.90–63.60
	36	66.56–80.01	89.56 - 92.44	72.93–83.60	93.40–96.13	75.38 - 81.28	59.84–68.91	61.30–78.34
	48	80.35–89.50	93.20 - 96.70	75.14–92.52	98.23–100.00	80.25–90.34	70.26–83.40	69.18–85.60

[a] Values in each row and column represent the minimum and the maximum biodegradation and reduction efficiency values (%) obtained from the isolates in each fungal groups.

degrade pollutants, bioremediation is widely regarded as one of the most promising approaches to remediate crude oil contamination [33]. Hence, the emphasis on boosting and recovery the natural microbial communities in this study to break down various hydrocarbons and crude oil in polluted environments is crucially important for the remediation of oil and hydrocarbon pollution.

3.3. The bioremoval efficiency of different emerging contaminants hazard pollutants from aqueous solutions by the indigenous mycobiome of the refinery wastewater in Jazan

The average bioremoval of the hazard materials including diclofenac, ibuprofen, carbamazepine, acetaminophen, sulfamethoxazole, bisphenol, bleomycin, vincristine, dicofol, methyl parathion, atrazine, diuron, dieldrin, chlorpyrifos, profenofos and phenanthrene by *Fusarium* isolates was estimated to be 74.0, 82.42, 49.88, 83.2, 70.9, 85.12, 70.15, 77.42, 90.33, 58.22, 100.0, 30.87, 90.0, 75.0, 100.0 and 48.16 %, respectively (Fig. 2). *Fusarium* species like *F. culmorum* have demonstrated the capability to degrade high concentrations (3 g/L) of toxic substances, including DEHP, as the sole carbon and energy source in solid-state fermentation (SSF) [34]. The biodegradation reached 96.9 % within 312 h, presenting an environmentally promising alternative that could aid in mitigating the adverse effects of environmental contamination by fungi. The *Verticillium* species exhibited the capability to eliminate these substances from their solutions, with average bioremoval percentages of 52.0, 49.77, 72.11, 75.13, 65.18, 80.19, 64.22, 88.0, 88.15, 80.75, 100.0, 45.23, 100.0, 90.0, 100.0 and 61.52, respectively (Fig. 2). El-Bondkly and El-Gendy et al. [4], offers important insights into critical using fungal bioremediation for both economically and environmentally transformation and detoxification of pollutants as sound solutions in the bio-refinery applications using the mycobiomes isolated from the refinery effluents.

The average values of bioremoval efficiency of hazard materials by the species of *Clavispora* and *Purpureocillium* of diclofenac (90.18 and 68.0 %), ibuprofen (55.3 and 72.21 %), carbamazepine (66.17 and 82.15 %), acetaminophen (54.39 and 80.0 %), sulfamethoxazole (78.44 and 90.11 %), bisphenol (90.77 and 84.36 %), bleomycin (69.88 and 85.9 %), vincristine (65.39 and 100.0 %), dicofol (48.16 and 61.93 %), methyl parathion (60.44 and 75.80 %), atrazine (100.0 and 100.0 %), diuron (70.12 and 50.76 %), dieldrin (68.19 and 67.23 %), chlorpyrifos (90.0 and 82.00 %), profenofos (100.0 and 100.0 %), and phenanthrene (60.73 and 82.93 %) were fruitful and promising for environmental applications (Fig. 2). Pollution is a global menace that poses harmful effects on all the living ecosystems and to the Earth. Although many treatments and processing strategies are waged for treating such pollutants, the fungal treatments of hazardous waste are innovative and long-lasting solutions required addressing the urgent global issue of hazardous pollutant remediation from contaminated environments [30]. Interestingly, among all fungal mycobiome under study, *Scedosporium* isolates showed the highest bioremoval efficiency against all hazard materials under study (Fig. 2). Fungi are renowned for their remarkable capacity to degrade a wide array of organic compounds [35]. This ability through their distinctive oxidative and extracellular ligninolytic systems, which empower them to effectively transform or break down various environmental contaminants, including polycyclic aromatic hydrocarbons (PAHs), pharmaceuticals, endocrine-disrupting compounds (EDCs), pesticides, synthetic dyes, and other pollutants.

The total bioremoval efficiency (100.0 % bioremoval) by the six isolates belongs to *Scedosporium* was recorded for bisphenol, bleomycin, vincristine, dicofol, atrazine, dieldrin, chlorpyrifos and profenofos materials followed by diclofenac (96.13 %), phenanthrene (94.18 %), sulfamethoxazole (93.16 %), carbamazepine (91.5 %), methyl parathion (91.37 %), ibuprofen (89.72 %), acetaminophen (89.66 %) and diuron (89.60 %) (Fig. 2). Myco-remediation is a top-down green and eco-friendly tool for pollution management beside it is a cost-effective and safer practice of converting pernicious substances into non-toxic forms by the use of fungi

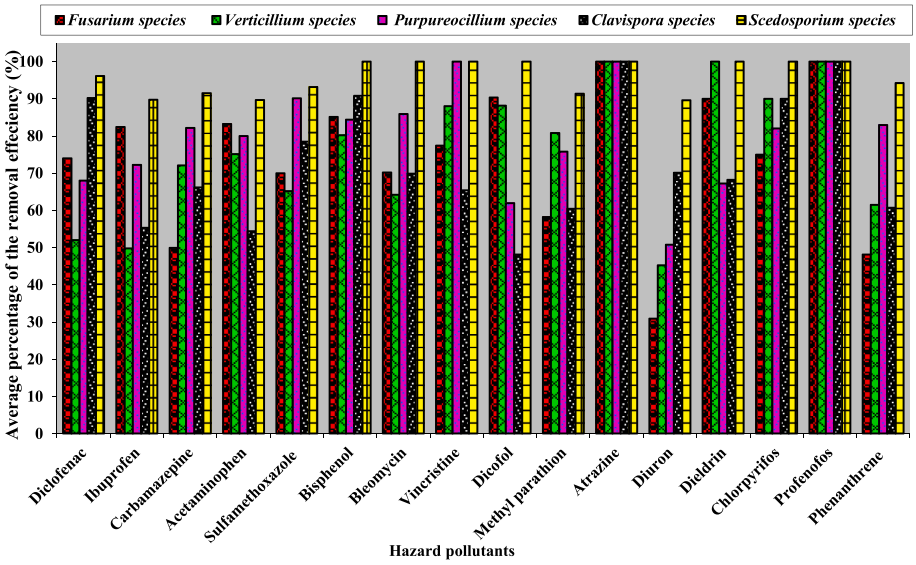

Fig. 2. The bioemoval efficiency (%) of different hazard pollutants from aqueous solutions by the indigenous mycobiome of the refinery wastewater. Each adsorption value is the average value of bioemoval obtained from the isolates of each genus.

that can transform these pollutants into useable products along with multiple benefits for the environment such as sequestration of carbon emissions and also to generate high valuable bioactive materials that fits as a sustainable economic model [36].

3.4. Evaluation of IC_{50} and MICs values of different heavy metals against mycobiome derived from the refinery wastewater in Jazan and their bioremoval from aqueous solutions

Contamination with heavy metals (HMs) poses a significant threat to biological systems, given their non-biodegradable and persistent nature, which undermines environmental safety and human health. The spectrum of HMs resistance to HMs within the isolated fungal community was investigated on PDA medium to assess their ability to withstand stress induced by a multimetals aqueous solution containing Fe^{2+}, Ni^{2+}, Cr^{6+}, Zn^{2+}, As^{3+}, Cu^{2+}, Cd^{2+}, Pb^{2+}, Hg^{2+} and Ag^{+}, individually. It was not surprising that all of the fungal isolates exhibited moderate to high levels of resistance for these heavy metals (Table 3). The spectrum of HMs resistance (IC_{50} and MIC) within the *Fusarium* species was primarily directed to Zn^{2+} (2.31–2.47 and 4.00–4.32), followed by Pb^{2+} (1.65–2.00 and 2.80–3.62), Fe^{2+} (1.32–1.61 and 2.30–2.90), Cd^{2+} (1.22–1.55 and 2.20–2.72), As^{3+} (1.18–1.50 and 2.00–2.61), Cr^{6+} (1.00–1.30 and 1.95–2.50), Ag^{+} (0.77–1.00 and 1.60–1.80), Cu^{2+} (0.32–0.57 and 0.96–1.11), Ni^{2+} (0.30–0.61 and 0.87–0.96), and Hg^{2+} (0.25–0.50 and 0.59–0.93) g/L, respectively (Table 3). In the process of remediating heavy metals (HMs), fungi are commonly employed in their live, viable state. This necessitates them to possess a degree of tolerance to pollutants since these substances are often inherently toxic and can hinder fungal growth [37]. Researchers have identified a diverse range of fungi capable of reducing HMs from wastewater. These fungi encompass species such as *Fusarium*, *Verticillium Aspergillus*, *Trichoderma*, *Penicllium*, *Beauveria*, *Mucor*, *Clavispora*, *Trichoderma*, *Phanerochaete*, *Purpureocillium* and *Simplicillium* species. They have demonstrated potential tolerance and

Table 3
Evaluation of IC_{50s} and MICs values (g/L) of different heavy metals against mycobiome derived from the refinery wastewater mycobiome of the industrial area of Jazan and their removal capacity (%) from aqueous solutions.

Heavy metals	Fungal group, (IC_{50} and MIC value g/L)[a] and adsorption efficiency (RE%)				
	Fusarium sp.	*Verticillium* sp.	***Clavispora* sp.**	*Purpureocillium* sp.	*Scedosporium* sp.
Fe^{2+}					
IC_{50}	1.32–1.61	1.60–2.25	0.90–1.16	1.50–1.87	2.75–3.12
MIC	2.30–2.90	2.19–3.27	1.70–3.18	2.34–2.86	4.00–5.39
RE	55.64–70.05	37.93–65.70	29.13–41.22	42.30–65.90	70.17–90.8
Ni^{2+}					
IC_{50}	0.30–0.61	1.00–1.30	0.46–0.91	1.18–160	1.60–1.90
MIC	0.87–0.96	1.70–2.30	0.68–1.70	2.15–2.62	2.79–3.15
RE	29.23–54.78	70.62–76.48	33.56–60.90	60.87–76.96	83.45–96.13
Cr^{6+}					
IC_{50}	1.00–1.30	0.30–0.60	1.47–2.00	1.50–2.70	1.68–2.10
MIC	1.95–2.50	0.62–0.90	2.50–3.00	1.40–4.00	3.30–4.00
RE	80.11–100.00	50.29–68.91	43.69–60.15	61.95–82.50	89.84–100.00
Zn^{2+}					
IC_{50}	2.31–2.47	1.52–1.73	1.12–1.30	1.16–1.84	2.00–2.60
MIC	4.00–4.32	2.10–2.95	2.00–2.73	2.27–3.50	3.92–4.37
RE	70.80–89.37	60.33–78.10	11.70–46.30	74.00–86.32	75.16–93.60
As^{3+}					
IC_{50}	1.18–1.50	1.18–1.49	1.70–2.05	1.19–1.42	1.93–2.29
MIC	2.00–2.61	1.98–2.20	2.60–3.76	1.50–2.18	3.23–4.15
RE	63.14–78.45	58.45–73.61	30.25–45.19	32.00–69.61	85.72–100.00
Cu^{2+}					
IC_{50}	0.32–0.57	0.65–0.97	1.15–2.16	0.48–0.60	1.80–2.44
MIC	0.96–1.11	1.25–1.83	2.20–3.62	1.00–1.76	2.50–3.70
RE	39.51–50.39	76.12–80.37	55.28–77.63	60.96–71.11	86.50–100.00
Cd^{2+}					
IC_{50}	1.22–1.55	0.35–0.74	0.86–1.20	1.20–1.53	1.80–2.41
MIC	2.20–2.72	0.68–1.52	1.59–2.15	2.00–3.12	3.21–4.17
RE	48.32–72.70	30.22–54.21	31.44–60.32	79.20–85.72	72.95–96.31
Pb^{2+}					
IC_{50}	1.65–2.00	0.93–1.22	0.41–0.56	0.84–1.52	1.55–1.80
MIC	2.80–3.62	1.78–2.61	0.86–1.19	2.15–2.89	2.28–3.42
RE	80.04–92.18	47.50–70.81	23.70–50.27	54.80–73.62	82.80–98.00
Hg^{2+}					
IC_{50}	0.25–0.50	0.37–0.60	0.68–1.00	1.12–1.61	1.60–2.00
MIC	0.89–1.13	0.65–1.35	1.09–1.79	2.00–3.12	2.10–3.70
RE	44.26–60.00	39.88–73.19	10.78–49.00	69.59–80.93	70.68–100.00
Ag^{+}					
IC_{50}	0.77–1.00	1.23–1.70	0.49–0.80	1.40–1.80	1.70–1.95
MIC	1.60–1.80	1.99–2.25	0.97–1.50	2.36–3.49	3.00–4.17
RE	39.52–64.94	57.23–74.38	21.35–30.28	71.60–92.60	80.42–95.62

[a] The IC_{50}, MIC and adsorption efficiency values are the maximum and minimum values obtained from the isolates of each fungal group of at least three independent measurements.

remediation abilities towards various HMs, including lead, cadmium, chromium, iron, copper, cobalt, nickel, zinc, and manganese, found in contaminated wastewater. These fungi are characterized as multi-metal-adsorptive fungi [5,38–41]. Furthermore, Table 3 indicated that *Verticillium* species showed the highest IC_{50} and MIC values against Fe^{2+} (1.60–2.25 and 2.19–3.27 g/L) followed by Zn^{2+} (1.52–1.73 and 2.10–2.95 g/L), Ag^{+} (1.23–1.70 and 1.99–2.25 g/L), and As^{3+} (1.18–1.49 and 1.98–2.20 g/L), respectively while *Clavispora* species exhibited higher resistant values toward As^{3+} followed by Cr^{6+} and Cu^{2+} (IC_{50} = 1.70–2.05, 1.47–2.00 and 1.15–2.16 g/L with MIC values 2.60–3.76, 2.50–3.0 and 2.20–3.62 g/L, respectively). Consistent with our findings, Văcar et al. documented significant variations in the MIC values of heavy metals among numerous fungal strains. For example, *Fusarium oxysporum* P2.5 and P2.7 isolates had MIC values (mg/L) of 140 and 200 for Hg^{2+}, 2353 and 2092 for Zn^{2+}, and 1568 for Pb^{2+}; *Phoma costariensis* P2.10 and *Cladosporium* sp. TRD3.2 had Hg^{2+} MIC values of 160 and *Sarocladium kiliense* P2.2 presented MIC values of 200 for Hg^{2+}, 1036 for Pb^{2+}, and 381 for Cu^{2+} while *S. kiliense* TRD5P.6 showed MICs 337 and 160 for Cd^{2+} and Hg^{2+}, respectively [42].

Interestingly data in Table 3 showed that, *Purpureocillium* species presented IC_{50} and MIC values 1.5 to 2.7 and 1.4–4.0 g/L for Cr^{6+}, 1.16–1.84 and 2.27–3.5 g/L for Zn^{2+}, 1.4–1.8 and 2.36–3.49 g/L for Ag^{+}. Hence, it was noted that while the resistance profiles to heavy metals are present across all fungal populations, the extent of resistance can vary uniquely among species. El-Gendy et al., recorded the MICs of the heavy metals; Cu^{2+} and Cd^{2+} against different fungi derived from heavy metals contaminated areas including *Rhizopus oryzea* (200 and 716 μg/mL), *Aspergillus luchuensis* (417 and 590 μg/mL), *Aspergillus tubingensis* (350 and 280 μg/mL), *Monacrosporium elegans* (630 and 800 μg/mL), *Penicillium duclauxi* (299 and 630 μg/mL), *Curvularia lunata* (214 and 400 μg/mL), *Penicillium lilacinum* (1000 and 650 μg/mL), *Drechslera hawaiiensis* (950 and 290 μg/mL), *Verticillium Fungicola* (318 and 512 μg/mL) and *Pestalotiopsis clavispora* (890 and 480 μg/mL). Overall, *Scedosporium* species exhibited the highest resistance to multiple heavy metals, as evidenced by the highest IC_{50} values. (2.75–3.12, 1.6–1.9, 1.68–2.1, 2.0–2.6, 1.93–2.29, 1.8–2.44, 1.8–2.41, 1.55–1.8, 1.6–2.0 and 1.7–1.95 g/L) along with the highest MIC values (4.0–5.39, 2.79–3.15, 3.3–4.0, 3.92–4.37, 3.23–4.15, 2.5–3.7, 3.21–4.17, 2.28–3.42, 2.1–3.7 and 3.0–4.17 g/L) against Fe^{2+}, Ni^{2+}, Cr^{6+}, Zn^{2+}, As^{3+}, Cu^{2+}, Cd^{2+}, Pb^{2+} Hg^{2+} and Ag^{+}, respectively (Table 3). In this study, the resistance of fungi isolated from refinery effluents to Fe^{2+} was found to be correlated with resistance to other heavy metals, suggesting significant potential for the development of bioremediation strategies targeting substrates or sites contaminated with multiple heavy metals. Previous studies highlighted the robust metabolic capabilities of the environmental isolate of *S. apiospermum* in interacting with contaminated environments. Furthermore, this study represents the first documentation of the effectiveness of dead biomass from *Scedosporium* strain in the bioremoval and adsorption of heavy metals from the industrial wastewater [43,44].

3.5. Bioremoval efficiency of heavy metals from the multimetals aqueous solution by the mycobiota of refinery wastewater

The ten isolates of *Fusarium* demonstrated the capability to remove heavy metals such as Fe^{2+}, Ni^{2+}, Cr^{6+}, $Zn^{2+,}$ As^{3+}, $Cu^{2+,}$ Cd^{2+}, Pb^{2+}, Hg^{2+} and Ag^{+} from a multi-metals aqueous solution containing equal concentrations of these heavy metals (total concentration 3 g/L, 300 mg/L for each). The removal rates ranged from 55.64 % to 70.05 % for Fe^{2+}, 29.23 %–54.78 % for Ni^{2+}, 80.11 %–100.0 % for Cr^{6+}, 70.8 %–89.37 % for $Zn^{2+,}$ 63.14 %–78.45 % for As^{3+}, 39.51 %–50.39 % for Cu^{2+}, 48.32 %–72.7 % for Cd^{2+}, 80.04 %–92.18 % for Pb^{2+}, 44.26 %–60.0 % for Hg^{2+} and 39.52 %–64.94 % for Ag^{+}, respectively (Table 3). In line with our findings, El-Bondkly and El-Gendy, documented the effectiveness of the mycobiome derived from Mostorod and Tanta refineries in Egypt for optimal removal heavy metals and polycyclic aromatic hydrocarbons from aqueous solutions [4]. Various *Fusarium* strains have demonstrated adaptation to elevated concentrations of heavy metals such as Co, Cu and Mn, suggesting their potential use as natural biosorbents for remediating heavy metals from aqueous solutions and polycyclic aromatic hydrocarbon (PAH)-contaminated soil, particularly in coal mining areas.

As shown in Table 3, *Verticillium* species showed powerful bio-remediation ability toward Fe^{2+} (37.93–65.7 %), Ni^{2+} (70.62–76.48 %), Cr^{6+} (50.29–68.91 %), Zn^{2+} (60.33–78.1 %), As^{3+} (58.45–73.61 %), Cu^{2+} (76.12–80.37 %), Cd^{2+} (30.22–54.21 %), Pb^{2+} (47.5–70.81 %), Hg^{2+} (39.88–73.19 %), and Ag^{+} (57.23–74.38 %). Feng et al. highlighted the effective degradation of pesticides like chlorpyrifos and the efficient biosorption mechanism for Pb^{2+} and Zn^{2+} by *Verticillium* species. They emphasized the potential utilization of these species for the development of biotreatment technologies targeting heavy metal-polluted waste [45]. The biomass of *Clavispora* species demonstrated lower removal efficiency, ranging from 29.13 % to 41.22 % for Fe^{2+}, 33.56 %–60.9 % for Ni^{2+}, 43.69 %–60.15 % for Cr^{6+}, 11.7 %–46.3 % for Zn^{2+}, 30.25 %–45.19 % for As^{3+}, 55.28 %–77.63 % for Cu^{2+}, 31.44 %–60.32 % for Cd^{2+}, 23.7 %–50.27 % for Pb^{2+}, 10.78 %–49.0 % for Hg^{2+}, and 21.35 %–30.28 % for Ag^{+} (Table 3). Additionally, germinated spores and dead insoluble cell walls of microbiome strains, including *Mucor hiemalis* exhibited multimetals-resistance, hyper-accumulation, and elicitation power for effectively removing >81 %–99 % of Al, Cd, Co, Cr, Cu, Hg, Ni, Pb and Zn simultaneously and enriched precious metals from water all in 48 h [46].

Fruitful bioremoval activity ranges equal to 42.3–65.90 % of Fe^{2+}, 60.87–76.96 % of Ni^{2+}, 61.95–82.5 % of Cr^{6+}, 74.0–86.32 % of Zn^{2+}, 32.0–69.61 % of As^{3+}, 60.96–71.11 % of Cu^{2+}, 79.2–85.72 % of Cd^{2+}, 54.8–73.62 % of Pb^{2+}, 69.59–80.93 % of Hg^{2+} and 71.6–92.6 % of Ag^{+} were achieved after treated the multi-metals solution with the dead biomass of *Purpureocillium* species (Table 3). The advancement in bioremediation utilizing filamentous fungi has become the main issue to addressing contemporary challenges in pharmaceutical compound, heavy metal, and oil hydrocarbon remediation. The biological processes play a crucial role in wastewater treatment. Mycoremediation incorporates diverse cellular mechanisms employed by filamentous fungi for bioremediation purposes, such as bio-adsorption, bio-surfactant synthesis, bio-mineralization, bio-precipitation, as well as extracellular and intracellular enzymatic processes. Through these biological processes, mycoremediation contributes significantly to wastewater treatment efforts [47].

Among all fungal genera of petrol refining wastewater, the isolates belonged to the genus *Scedosporium* showed the highest bioremoval efficiency against all heavy metals under study (Table 3). The bioremoval efficiency of these heavy metals by the dead biomass

of *Scedosporium* was in the ranges of 70.17–90.8 % of Fe^{2+}, 83.45–96.13 % of Ni^{2+}, 89.84–100.0 % of Cr^{6+}, 75.16–93.6 % of Zn^{2+}, 85.72–100.0 % of As^{3+}, 86.5–100.0 % of Cu^{2+}, 72.95–96.31 % of Cd^{2+}, 82.8–98.0 % of Pb^{2+}, 70.68–100.0 % of Hg^{2+} and 80.42–95.62 % of Ag^{+} (Table 3). The extensive species diversity of filamentous fungi utilized in pollutant removal, encompassing prominent species like *Aspergillus*, *Penicillium*, *Fusarium*, *Verticillium*, *Phanerochaete* and other species from *Basidiomycota* and *Zygomycota* coupled with their efficiency in eliminating a wide range of pollutant compounds and their ease of handling, make them valuable tools for bioremediation efforts targeting emerging contaminants. Moreover, these fungi have the capacity to produce various beneficial byproducts such as chitosan, ethanol, lignocellulolytic enzymes, organic acids, and nanoparticles, further enhancing their utility in remediation processes [16].

3.6. Incidence of antifungal resistance among fungi derived from refinery wastewater

In this study, we investigated the sensitivity profiles of fungal isolates belonging to five genera groups including *Fusarium*, *Verticillium*, *Clavispora, Purpureocillium* and *Scedosporium* were examined against various classes of antibiotics to various classes of antibiotics. These included azoles (fluconazole, itraconazole, voriconazole, posaconazole, isavuconazole and ketoconazole), echinocandins (anidulafungin, caspofungin and micafungin) and polyenes (amphotericin B) drugs. Minimum inhibitory concentrations (MICs) and minimum fungicidal concentrations (MFCs) were determined (Table 4) to assess their sensitivity to commonly used antibiotics. This analysis aimed to prevent the spread of multidrug resistance in the environment and ensure that the selected fungi, used as biosorbents for hydrocarbons and heavy metals in environmental remediation, are susceptible to antibiotics.

Several species of molds including *Fusarium*, *Verticillium*, *Clavispora*, *Purpureocillium* and *Scedosporium* species have reduced susceptibility or pan-resistance to clinically available antifungals [7]. Data in Table 4 showed that among azoles drugs against *Fusarium*, *Verticillium*, *Clavispora*, *Purpureocillium* and *Scedosporium* species, the highest resistance toward fluconazole was detected in the isolates of *Fusarium* species (MIC = 100–200, MFC = 128–250 μg/mL) followed by *Clavispora* (MIC = 40–100, MFC = 64–125 μg/mL), *Purpureocillium* (MIC = 32–64, MFC = 48–96 μg/mL) and *Verticillium* (MIC = 28–56, MFC = 40–80 μg/mL), but the highest sensitivity against fluconazole was detected in isolates of *Scedosporium* group (MIC = 16–32, MFC = 24–40 μg/mL) (Table 4). MICs in the range of 32–100, 20–36, 16–32, 12–32 and 12–20 μg/mL with MFCs 64–200, 40–64, 32–60, 20–40 and 16–32 μg/mL of itraconazole were

Table 4
Incidence of antibiotic resistant among the fungal mycobiota derived from the petroleum refining wastewater.

Antifungal drugs	Fungal group, MIC/MFC ranges (μg/mL)				
	Fusarium sp.	Verticillium sp.	Clavispora sp.	Purpureocillium sp.	Scedosporium sp.
Azole antibiotics					
Fluconazole					
MIC	100.0–200.0	28.0–56.0	40.0–100.0	32.0–64.0	16.0–32.0
MFC	128.0–250.0	40.0–80.0	64.0–125.0	48.0–96.0	24.0–40.0
Itraconazole					
MIC	32.0–100.0	12.0–32.0	20.0–36.0	16.0–32.0	12.00–20.0
MFC	64.0–200.0	20.0–40.0	40.0–64.0	32.0–60.0	16.0–32.0
Voriconazole					
MIC	16.0–64.0	4.0–12.0	4.0–16.0	4.0–64.0	4.0–8.0
MFC	80.0–128.0	24.0–64.0	28.0–80.0	48.0–96.0	12.0–20.0
Posaconazole					
MIC	28.0–96.0	12.0–32.0	16.0–64.0	16.0–32.0	8.0–10.0
MFC	64.0–128.0	20.0–64.0	32.0–128.0	24.0–80.0	12.0–16.0
Isavuconazole					
MIC	16.0–24.0	4.0–10.0	8.0–20.0	4.0–16.0	4.0–8.00
MFC	40.0–48.0	12.0–20.0	32.0–40.0	20.0–24.0	8.0–20.0
Ketoconazole					
MIC	32.0–128.0	16.0–24.0	24.0–64.0	20.0–40.0	4.0–10.00
MFC	64.0–200.0	32.0–64.0	60.0–128.0	48.0–100.0	10.00–16.00
Echinocandin antibiotics					
Anidulafungin					
MIC	16.0–64.0	4.0–32.0	16.0–32.0	8.0–32.0	4.0–28.0
MFC	24.0–128.0	28.0–100	16.0–64.0	16.0–128.0	12.0–36.0
Caspofungin					
MIC	32.0–100.0	8.0–32.0	24.0–64.0	24.0–64.0	8.0–32.0
MFC	64.0–150.0	16.0–64	32.0–128.0	32.0–160.0	8.0–56.0
Micafungin					
MIC	24.0–128.0	16.0–64.0	18.0–32.0	23.0–80.0	8.0–16.0
MFC	80.0–256.0	32.0–128	32.0–80.0	28.0–96.0	10.0–24.0
Polyenes antibiotics					
Amphotericin B					
MIC	8.0–10.0	4.0–8.0	4.0–16.0	8.0–12.0	2.00–4.00
MFC	8.0–32.0	4.0–24.0	20.0–48.0	16.0–24.0	4.00–8.00

* The MIC and MFC values are the maximum and minimum values obtained from the isolates of each fungal group of at least three independent measurements.

detected against *Fusarium*, *Clavispora*, *Purpureocillium*, *Verticillium* and *Scedosporium* species, respectively (Table 4). However, the lowest MIC and MFC values of posaconazole, isavuconazole and ketoconazole were recorded for the species *Scedosporium* followed by *Verticillium*, *Purpureocillium*, *Clavispora*, and *Fusarium* species, respectively (Table 4). The resistance to fluconazole and itraconazole poses a significant concern in non-Candida fungal species, mainly because of the rising occurrences of infections attributed to these species across various geographical regions globally. Moreover, there is a growing prevalence of resistance to these widely utilized azoles in numerous institutions [48].

Isolates of *Fusarium* group showed the highest resistant against voriconazole with MIC = 16–64 and MFC 80–128 μg/mL while Isolates of *Scedosporium* group exhibited the highest sensitivity with MIC = 4–8 and MFC 12–20 μg/mL (Table 4). Resistance to azole antifungal agents among fungi has been observed globally, attributed to both clinical and environmental exposure to this class of agents. Such resistant isolates have been associated with invasive infections characterized by high mortality rates [49]. In accordance with our findings, Dimitrios et al. and Arendrup et al. have indicated that resistance to fluconazole may imply resistance to other azoles as well [49,50]. This is due to mechanisms that diminish susceptibility to fluconazole, such as point mutations within the ERG11 gene, which encodes lanosterol 14α-demethylase, the target enzyme of azoles (e.g., itraconazole, voriconazole, posaconazole, and isavuconazole). These mechanisms can increase transcription of the ERG11 gene, resulting in elevated levels of the enzyme, or involve efflux pumps such as Cdr1 and Cdr2, which also impact this class of antifungals [51]. The MICs and MFCs of echinocandins drugs were determines against *Fusarium* group (MICs; 16–64, 32–100 and 24–128 μg/mL with MFCs; 24–128, 64–150 and 80–256 μg/mL), *Verticillium* group (MICs; 4–32, 8–32 and 16–64 μg/mL with MFCs; 28–100, 16–64 and 32–128 μg/mL), *Clavispora* group (MICs; 16–32, 24–64 and 18–32 μg/mL with MFCs; 16–64, 32–128 and 32–80 μg/mL), *Purpureocillium* group (MICs; 8–32.0, 24–64 and 23–80 μg/mL with MFCs; 16–128, 32–160 and 28–96 μg/mL) and *Scedosporium* group (MICs; 4–28, 8–32 and 8–16 μg/mL with MFCs; 12–36, 8–56 and 10–24 μg/mL) against anidulafungin, caspofungin and micafungin, respectively (Table 4). Previously, Elizondo-Zertuche et al., proved that voriconazole and posaconazole exhibited excellent in vitro activity for most species while amphotericin B and fluconazole demonstrated limited antifungal activity and all of the strains were resistant to echinocandins [7].

Moreover, MICs and MFCs of amphotericin B were relatively lower for *fungal strains* under study. The species of *Fusarium*, *Verticillium*, *Clavispora*, *Purpureocillium* and *Scedosporium* had MICs 8–10, 4–8, 4–16, 8–12 and 2–4 μg/mL along with MFCs equal to 8–32, 4–24, 20–48, 16–24 and 4–8 μg/mL, respectively (Table 4). The dissemination of antibiotic resistance genes into the environment stands as a significant contributor to the escalating prevalence and dissemination of multidrug-resistant pathogens, posing a clinical challenge that is increasingly prevalent globally [16]. Notably, in the current study all *Scedosporium* isolates derived from refinery industry effluents in Jazan exhibited inherently minimal antifungal resistance to all azole, echinocandin and polyene drugs examined. Among these isolates, strain JAZ-20 was chosen for further investigation, including phylogenetic analysis, toxicity profiling, GC/MS analysis, and optimization of bioremoval process parameters. The selection of isolate JAZ-20 was based on several factors: i) it represents the first documented instance in Saudi Arabia of environmental distribution and antifungal susceptibility of *Scedosporium*; ii) it demonstrated superior efficiency in removing various hazardous pharmaceuticals and agrochemical pollutants; iii) it displayed the

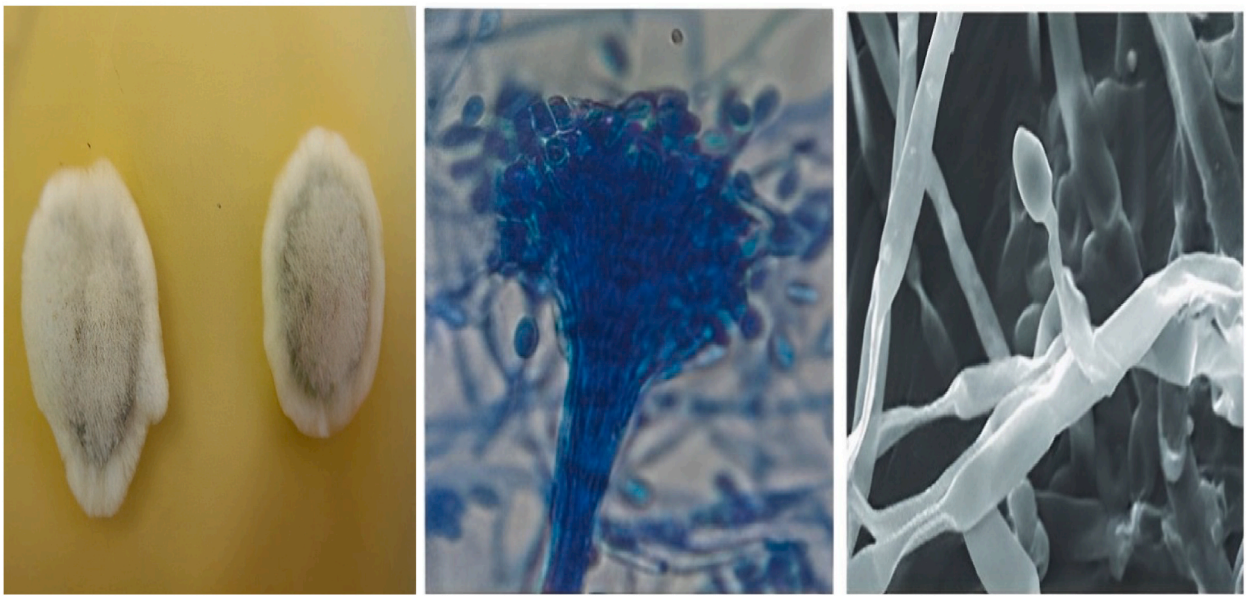

Fig. 3. Photomicrograph of colony characteristics (a), microscopic morphology; (b), lactophenol cotton blue magnification × 400) showing solitary and cylindrical conidiophores with graphium morphology of *S. apiospermum* (b) and scanning electron microscopy (c, the scale is 10 μm) showing cylindrical, thin and septate hyphae, globose to subglobose thick-walled large conidia with a diameter 8–10 × 4–6 μm.

highest tolerance to heavy metals and exhibited remarkable removal capabilities among the fungal strains studied; iv) it exhibited the lowest MIC and MFC against all antifungal agents tested, in addition to its heightened bioremediation activity towards hydrocarbons and crude oils.

3.7. Biochemical and morphological characteristics of the selected fungus Scedosporium sp. JAZ-20

On malt-yeast extract-agar medium (MYA), fungal strain JAZ-20 exhibited unique morphologies, characterized by colonies with colonies that were slightly oval in shape, with a hairy to cottony texture and a slightly raised. The upper view of these colonies appeared smoky grey with a creamy edge, while the reverse view displayed a dark tan coloration. After 5 days of incubation at 25 °C, these colonies expanded to a diameter ranging from 50 to 60 mm (Fig. 3a, Table 1). Microscopic examination of JAZ-20 strain using lactophenol cotton blue method and scanning electron microscopy (Fig. 3b and c) showed thin and septate hyphae with large end apical; solitary and cylindrical conidiophores with cylindrical graphium morphology, ovoid to ellipsoidal pale brown thick-walled conidia with size of 8.22–10.1 × 3.98–5.98 μm were observed. Graphium were133–340 μm consist of erect bundles of terminating hyphae in a brush of conidiogenous cells (Fig. 3 b, c; Table 1). For biochemical analysis in Table 5, it was able to utilize ribitol, L-arabinitol, sucrose and maltose but not D-ribose. It was able to grow at temperature ranged between 15 and 42 °C along with pH range 5–11 while it grew best at 35 to 37 °C and pH 8–9. It can tolerate NaCl up to 10 % (Table 4). Munoz et al. and Cortez et al. have previously described *S. apiospermum* isolates as typically exhibiting floccose, grey to brown colonies with synanamorph graphium, and the absence of cleistothecia in aged cultures [52,53]. Consistent with our findings, Kitisin et al. reported that *Scedosporium* isolates can be identified by their colonies, which are dark grey to smoke brown on the upper surface and dark olive green, brown, or black on the underside along with septate hyphae and solitary conidiophores producing pale brown, ovoid, or ellipsoidal conidia, with an average size of 8.18 ± 0.16 μm, and optimal growth at 37 °C [27].

Regarding the fatty acid profile of the chosen strain JAZ-20, the data presented in Table 5 illustrated that the composition of fatty acids included $C_{11:0}$ (0.12 %), $C_{14:0}$ (1.95 %), iso-$C_{14:0}$ (2.98 %), anteiso-$C_{14:0}$ (2.13 %), iso-$C_{15:0}$ (9.16 %), anteiso-$C_{15:0}$ (11.75 %), $C_{15:0}$ (7.42 %), $C_{15:1}$ (2.37 %), anteiso-$C_{16:0}$ (3.4 %), $C_{16:0}$ (10.3 %), iso-$C_{16:0}$ (9.5 %), $C_{17:1}$ (1.36 %), anteiso-$C_{17:1}$ (8.64 %), iso-$C_{18:0}$ (11.0 %), $C_{18:0}$ (3.63 %), $C_{18:1\ w9}$ (0.65 %), anteiso-$C_{19:0}$ (3.78 %), $C_{19:1}$ (0.8 %), anteiso-$C_{20:0}$ (2.0 %), iso-$C_{21:0}$ (2.44 %), $C_{23:0}$ (1.15

Table 5
Biochemical and morphological characterization of the selected fungal strain JAZ-20.

Phenotypic character	Result
Assimilation of	
Ribitol	+
L-Arabinitol	+
Sucrose	+
Maltose	+
D-Ribose	–
Temperature range	15 - 42 °C
Optimum temperature	35-37 °C
NaCl tolerant	up to 10 %
pH range	5–11
Optimum pH	8–9
Fatty acid profile	
$C_{11:0}$	(0.12)
$C_{14:0}$	(1.95)
Iso-$C_{14:0}$	(2.98)
Anteiso - $C_{14:0}$	(2.13)
Iso-$C_{15:0}$	(9.16)
Anteiso-$C_{15:0}$	(11.75)
$C_{15:0}$	(7.42)
$C_{15:1}$	(2.37)
Anteiso-$C_{16:0}$	(3.40)
$C_{16:0}$	(10.30)
Iso-$C_{16:0}$	(9.50)
$C_{17:1}$	(1.36)
anteiso-$C_{17:1}$	(8.64)
Iso-$C_{18:0}$	(11.00)
$C_{18:0}$	(3.63)
$C_{18:1\ w9}$	(0.65)
Anteiso –$C_{19:0}$	(3.78)
$C_{19:1}$	(0.80)
Anteiso-$C_{20:0}$	(2.00)
Iso-$C_{21:0}$	(2.44)
$C_{23:0}$	(1.15)
$C_{24:0}$	(2.17)
$C_{26:0}$	(0.38)
$C_{27:0}$	(0.92)

%), $C_{24:0}$ (2.17 %), $C_{26:0}$ (0.38 %), and $C_{27:0}$ (0.92 %). El-Gendy et al., mentioned that under harsh conditions as in the industrial effluents, especially from refineries, which contain a large numbers of toxicants the branched fatty acid such as iso-$C_{14:0}$, anteiso-$C_{14:0}$, iso-$C_{15:0}$, anteiso-$C_{15:0}$, anteiso-$C_{16:0}$, iso-$C_{16:0}$, anteiso-$C_{17:1}$, iso-$C_{18:0}$, anteiso- $C_{19:0}$, anteiso-$C_{20:0}$, and iso-$C_{21:0}$. The fatty acids play crucial roles in the survival of fungi, *Actinomycetes* and bacteria by exerting inhibitory effects on fungal growth and by eliminating or hindering the production of mycotoxins. Consequently, the strain under study produced these fatty acids in its challenging environment to facilitate its growth and competitive interactions with other organisms.

3.8. Molecular identification and phylogenetic analysis of selected fungus Scedosporium sp. JAZ-20

Following phenotypic identification, molecular analysis validated that the identified fungus strain JAZ-20 belongs to the species *Scedosporium apiospermum*. The amplification of the ITS region resulted in a single product (550 bp) for the isolate JAZ-20. The GenBank accession number of the ITS sequence of this fungal isolate is PP393523. A BLAST analysis performed via blastn search through GenBank displayed that the fungal isolate JAZ-20 belonged to division *Ascomycota*, class *Sordariomycetes*, order *Microascales*, family *Microascaceae*. Isolate JAZ-20 belonged to genus *Scedosporium* was clustered to those of accession numbers MT279294, MH911383, and KP132638 of the fungus *S. apiospermum* PUb 002, *S. boydii* MF 22543, and *S. apiospermum* SA2 an average pair wise similarity of 98.26, 98.24 and 98.07 %, respectively (Fig. 4). On its own, the morphological features used to identify specie of selected fungus *Scedosporium* sp. JAZ-20 did not allow differentiation of the present isolate and thus it was necessary to compare this data with molecular phylogeny. The alignments and phylogenetic analysis confirmed the taxonomic identity of selected fungus *Scedosporium* sp. JAZ-20 with *S. apiospermum*. Consequently, based on these criteria, *Scedosporium* sp. JAZ-20 fungal isolate could be recognized and designated as *Scedosporium apiospermum* JAZ-20. The most prominent fungal phylogenetic markers are the ITS region of the nuclear rDNA, 28 S and the 18 S rRNA genes sequences [54]. Furthermore, the molecular identification findings regarding the JAZ-20 strain align with the molecular identification of *Scedosporium* complex isolates from sites with significant human activity in Mexico, as reported by Elizondo-Zertuche et al., [7]. Consistent with our results, Gilgado et al. reported that the ecological study of *Scedosporium* complex isolates involved isolations from environmental sources, suggesting a preference for environments affected by human activity. Additionally, they noted that among *Scedosporium* species, *S. apiospermum* showed the highest prevalence (69 %), followed by S. boydii (16 %) [54].

3.9. Assessment of anti-proliferative activity of S. apiospermum JAZ-20 extract against human normal and adenocarcinoma cell lines

The cytotoxic effects of *S. apiospermum* JAZ-20 extract in Fig. 5 were evaluated across various concentrations on five distinct types of human normal cell lines; MCF10A, WI38, MRC5, HEK293, and HDFs. As illustrated in Fig. 5, cell death reaching 100 %, was induced in WI38, MRC5, MCF10A, HEK293, and HDFs cells upon treatment with JAZ-20 extract at doses of 30, 30, 40, 50 and 80 μg/mL, respectively. The corresponding IC_{50} values were 8.92, 10.41, 20.0, 16.5 and 40.0 μg/mL. Both WI38 and MRC5 human lung cells exhibited higher sensitivity to the JAZ-20 extract compared to the other cell lines. This heightened sensitivity may be attributed to the fact that, despite JAZ-20 being an environmental isolate, the primary route of infection by clinical isolates of *S. apiospermum* is through the lungs. Additionally, these fungi are acknowledged as frequent colonizers of the airways in individuals with cystic fibrosis [10]. Similarly, the data presented in Fig. 6 demonstrated complete suppression of proliferation in the human cancer cell lines HepG2, A549, and HeLa cells when treated with JAZ-20 extract at concentrations of 80, 60, and 70 μg/mL, respectively. The corresponding IC_{50} values were estimated to be 43.26, 33.75, and 40.0 μg/mL, respectively. In line with our results the microbial extract of different fungi

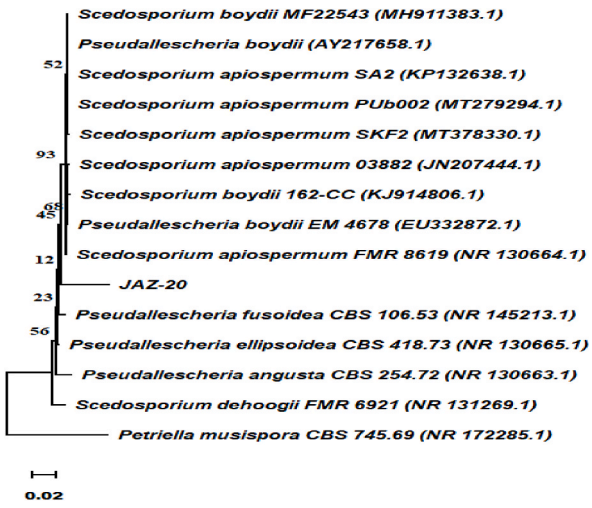

Fig. 4. Phylogenetic tree obtained from the ITS sequence data of the selected isolate JAZ-20 and sequences of reference strains obtained from GenBank, by neighbor-joining method.

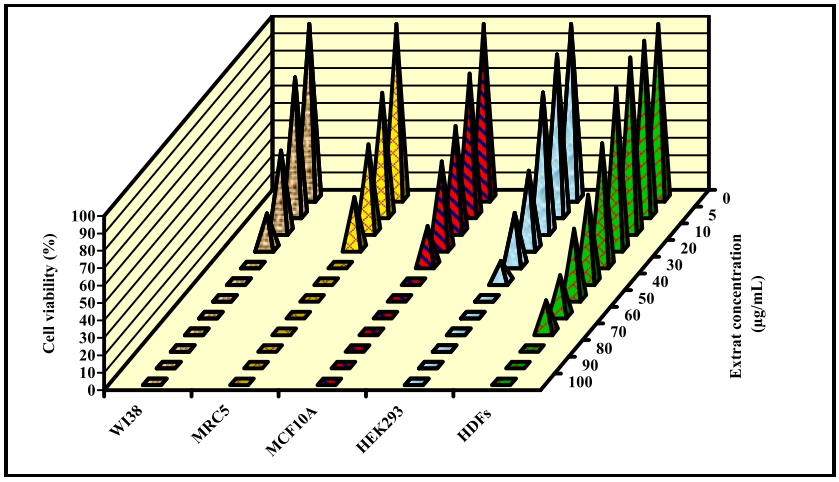

Fig. 5. Anti-proliferative activity of *S. apiospermum* JAZ-20 extract against different human normal cell lines.

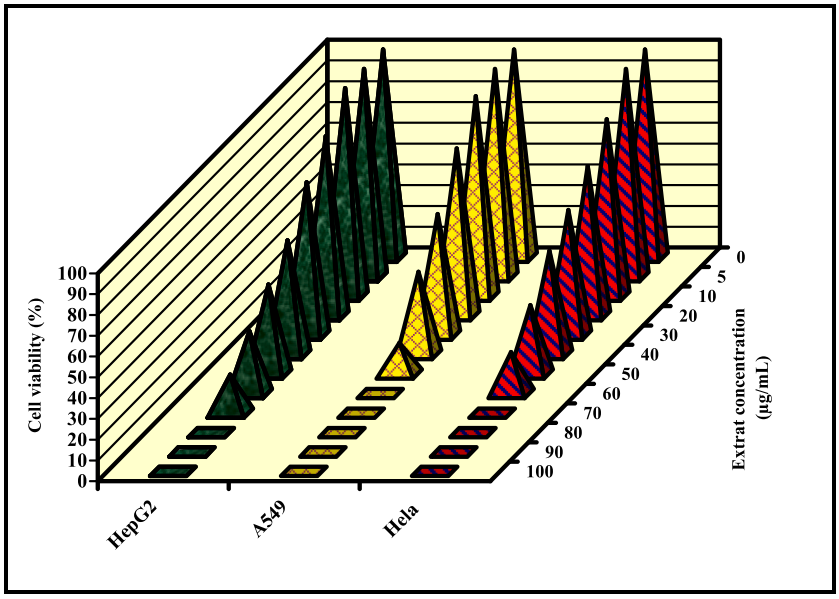

Fig. 6. Cytotoxic activity of *S. apiospermum* JAZ-20 extract against liver, lung and cervix human adenocarcinoma cell lines.

and *Actinomycetes* showed moderate to high cytotoxicity against different normal and caner cell lines in vitro studies [55–59]. Furthermore, in vivo studies confirmed that extracts from various Gram-negative and Gram-positive mycobiomes exhibited significant cytotoxic effects on liver and kidney cells in albino rats.

3.10. GC–MS analysis of the extract of S. apiospermum JAZ-20

The GC–MS of analysis of *S. apiospermum* JAZ-20 extract in Fig. 7 revealed a biochemical profile consisting of 47 volatile compounds (VOCs) spanning diverse chemical classes of secondary metabolites. These compounds exhibit various biological activities, including antifungal, antibacterial, antidiabetic, antiviral, anticancer, antioxidant and anti-inflammatory effects (Table 6 and Figs. 7, 8a-n). For instance, methane, a nitroso compound detected at a retention time of 6.19 (CH_3NO, peak area 1.52, M.W 45), previously isolated from fungi like *Muscodor albus* and recognized for its volatile DNA-methylating properties and its role as an antimicrobial and mycofumigation agent against a broad spectrum of human and plant pathogens. Remarkably, it can operate over a distance and diffuse through heterogeneous environments [60]. The titanium (IV) complexes, including tetraphenylporphyrinato dichlorotitanium and tetraphenylporphyrinato dibromotitanium, detected in the JAZ-20 extract at retention times of 7.29 and 45.3 min (Table 6, Fig. 8a and b), have garnered significant interest for their potential biological applications. They have been explored as antibiotics, biological sensors, tumor cell-killing agents, gene targeting devices, and antimicrobial agents due to their ability to generate reactive oxygen

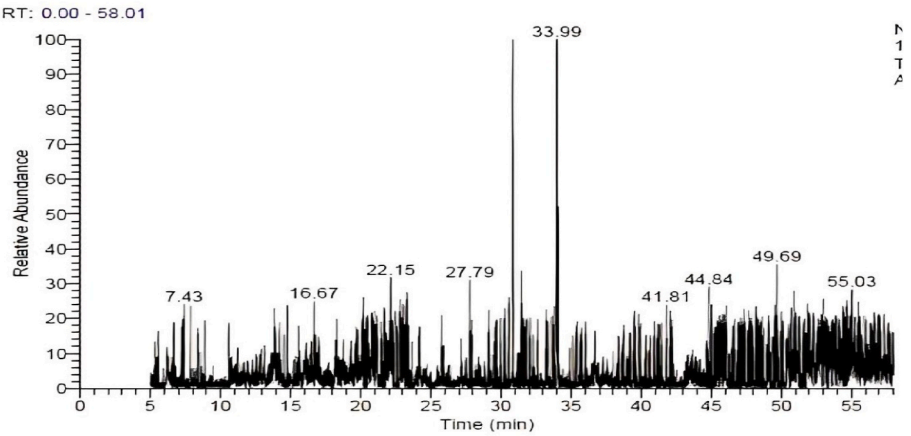

Fig. 7. GC/MS chromatogram of the extract of *S. apiospermum* JAZ-20 isolated from the industrial wastewater of refinery factories in the industrial area of Jazan.

species. These reactive oxygen species contribute to the decomposition of bacterial, fungal, algal, and viral cells owing to the oxophilic nature of these complexes and their ability to form strong bonds with various biological molecules [61]. Moreover, porphyrin-based compounds detected in the JAZ-20 extract such as 5,10-bis (3-aminophenyl)-15,20-diphenylporphyrin; 5,15-Bis(3-methoxyphenyl)-10-phenyl-20-propylporphyrin; 2-Methoxy-3-nitro-5,10,15,20-tetraphenyl-2,3-dihydroporphyrin and 2,4-bis(2-chloroethyl)-8--hydroxymethyl)-6,7-b is[2-(methoxycarbonyl) ethyl]-1,3,5-trimethylporphyrin detected at retention time 20.19, 33.25, 47.68 and 49.51 min (Table 6, Fig. 8c, d, e, f, respectively) play crucial roles in modern chemistry and biological processes. They serve as catalysts, light sensitizers, energy carriers, small molecule binders and carriers in the metabolism of living organisms [62]. Additionally, the detected compounds 5"-(1,1-Dimethylethyl)-2,2′,2″,2‴,2""-pentam ethoxy-[1,1':3′,1":3″,1‴:3‴.1""-quinquephenyl]-3,3""-dicarboxylic acid and *N,N′*-Dicyclohexyl-1,7- dipyrrolidinylperylene-3,4:9,10-tetracarboxylic acid bisimide were detected at retention times 47.88 and 51.21 min, respectively (Table 6, Fig. 8g and h). Godlewska-Żyłkiewicz et al., noted the biological activity of structure-related carboxylic acids such as antibacterial, antioxidant, and cytotoxic properties [63]. In the present study, compounds including anodendroside E 2, monoacetate (RT = 29.16, Table 6, Fig. 8i), hexadecanoic acid, methyl ester (RT = 30.85, Table 6, Figs. 8j), 9 and 12-octadecadienoic acid methyl ester, (E,E)-(CAS) (RT = 33.99, Table 6, Fig. 8k) were detected in the methylene chloride extract of JAZ-20 strain. These compounds previously identified by El-Sayed et al., in the methylene chloride extract of *Aspergillus sydowii* AUMC14506 with innovative anticancer, cytotoxic, and antibacterial modes of action [64]. Nickel (II) complexes such as (2-Nitro-5,10,15,20-tet raphenyl[2-(2)H1]prop hyrinato)nickel(II) (RT = 20.81, Table 6, Fig. 8l) and zinc (II) complexes such as (5,10,15,20-tetraphenyl[2-(2)H1]prophyrinato)zinc(II) and (2-hydroxy-5,10,15,20-t etraphenylporphinato)zinc(II) (Table 6, Fig. 8m) as well as copper(II) complexes (Table 6, Fig. 8n) detected in the current study have been reported as antioxidant, DNA-interacting, anti-inflammatory and anticancer agents [65–67].

3.11. Characterization the metal ions in the petroleum refining wastewater at Jazan city

The analysis of refinery wastewater collected from the industrial zone of Jazan, as presented in Table 7, revealed elevated toxic concentrations of four metal ions (Na^+, K^+, Ca^{2+} and Mg^{2+}) along with 14 heavy metals. The concentrations of these metal ions Na^+, K^+, Mg^{2+} and Ca^{2+} in the refinery wastewater were 3570.48 ± 10.42, 139.2 ± 1.12, 359.8 ± 2.57 and 560.93 ± 3.18, respectively which exceed allowable limit guidelines by 17.85, 13.92, 2.39 and 7.48-fold, respectively (Table 7). The concentration of heavy metals in descending order were detected to be Fe^{3+} (3015.68 ± 11.15 mg/L) > Mn^{2+} (267.52 ± 2.4 mg/L) > Co^{2+} (224.3 ± 2.51 mg/L) > Al^{3+} (185.17 ± 1.4 mg/L) > Ba^{2+} (166.37 ± 1.31 mg/L) > Pb^{2+} (41.15 ± 0.38 mg/L) > Zn^{2+}(35.31 ± 0.96 mg/L) > Ni^{2+} (27.46 ± 0.4 mg/L) > Cu^{2+} (19.92 ± 0.33 mg/L) > Cr^{6+} (7.9 ± 0.19 mg/L) > As^{3+} (3.13 ± 0.13 mg/L) > Ag^+ (3.0 ± 0.15 mg/L) > Cd^{2+} (2.27 ± 0.07 mg/L) > Hg^{2+} (0.130 ± 0.0 mg/L) (Table 7). In similar, El-Bondkly and El-Gendy et al., reported the abundance of the cations in the refinery wastewater collected from different industrial areas in Egypt in the order of $Na^+ > Fe^{3+} > Ca^{2+} > Mg^{2+} > Co^{2+} > Mn^{2+} > Ba^{2+} > Al^{3+} > K^+ > B^+ > Zn^{2+} > Pb^{2+} > Ni^{2+} > Cu^{2+} > As^{3+} > Cr^{6+} > Cd^{2+} > Ag^+ > Hg^{2+}$ [4]. However, upon comparing the concentrations of heavy metals found in petroleum refinery water in this study with the permissible limits outlined in WHO guidelines for water quality, it was observed that Fe^{3+} followed by Pb^{2+}, Hg^{2+}, Al^{3+}, Cd^{2+}, Mn^{2+}, Ni^{2+}, As^{3+} and Cr^{6+} are the elements with concentrations significantly surpassing the permissible limits. Specifically, their concentrations exceeded the limits by approximately 15078.4-, 4115-, 1030-, 925.85-, 756.66-, 535.04-, 392.29-, 313.0-, and 158.0-fold, respectively. Then these nine heavy metals were selected for the optimization studies of the bioremoval process parameters experiments from real petroleum refining wastewater (Table 7). The composition of a typical petroleum refinery wastewater typically based on the complication and routine pattern of the petroleum refining industry. Petroleum refinery wastewater is a complex mixture of oil and grease, organic pollutants include all BOD contaminants and inorganic pollutants include inorganic salts and heavy metals [68]. As a result, strategies for treating refinery wastewater are typically designed to effectively remove both organic and inorganic pollutants.

Table 6
Gas chromatography/mass spectrometry (GC/MS) analysis of the extract of *S. apiospermum* JAZ-20 isolated from the industrial wastewater of refinery factories in the industrial area of Jazan.

No.	Compound	Retention time (RT)	Peak area (%)	Molecular weight (g/mo)	Molecular formula
1	Methane, nitroso-	6.19	1.52	45	CH_3NO
2	tetraphenylporphyrinato dichlorotitanium(IV)	7.29	1.41	730	$C_{44}H_{28}Cl_2N_4Ti$
3	5,10-bis(3-aminopheny l)-15,20-diphenylporphyrin	20.19	1.52	644	$C_{44}H_{32}N_6$
4	1,3-Benzenedimethanol	20.40	1.50	500	$C_{16}H_{13}ClF_{12}O_2$
5	Nephthoside - 1,2′,3′,4′-Tetraacetate	20.50	3.35	696	$C_{40}H_{56}O_{10}$
6	(2-Nitro-5,10,15,20-tet raphenyl[2-(2)H1]prop hyrinato)nickel(II)	20 0.81	1.48	715	$C_{44}H_{27}N_5NiO_2$
7	3,3′-Bis[(5″-*tert*-butylsu lfanyl-2″-iodophenyl)et hynyl]tolane	21.51	1.88	806	$C_{38}H_{32}I_2S_2$
8	Benz[e]diacephenanthry lene[4,5-j:4′,5′-l]fluoranthene	22 0.14	1.59	600	$C_{48}H_{24}$
9	Dimethyl 2,anti-4,anti-9,12,anti14-pentabromodecacyc lo[9.9.0.0(1,8).0(2,12). 0 (6,10).0(11,18)0(13,1 7).0(16,20)] icosane-*syn*-4,syn-9-dicarboxylate	22.44	1.69	770	$C_{24}H_{23}Br_5O_4$
10	(2-hydroxy-5,10,15,20- tetraphenylporphinato)copper(II)	22.80	1.61	691	$C_{44}H_{28}CuN_4O$
11	[(Cyclopentadienyl)tris(diethylphosphito-P)cobalt-O,O′,O"]trichlorozirconium	22.96	2.44	730	$C_{17}H_{35}Cl_3CoO_9P_3Zr$
12	3(1),5(1)-cyclo-5(1)-(N -methylamino)-2,7,8,12,13,17,18-heptapropyl3(1)-ethyl-21H,23H-porphrin	23.13	1.61	685	$C_{46}H_{63}N_5$
13	5-(Dibromomethyl)-1,3-bis(tribromomethyl)benzene	24.21	1.50	744	$C_9H_4Br_8$
14	Anodendroside E2, monoacetate	29.16	1.89	616	$C_{32}H_{40}O_{12}$
15	4,4′,4″,4‴-Tetrabromote traphenylmethane	30.28	1.41	632	$C_{25}H_{16}Br_4$
16	Hexadecanoic acid, methyl ester (CAS)	30.85	6.99	270	$C_{17}H_{34}O_2$
17	5,5′-Bis[3-bromo-5-(methoxymethoxymethyl) phenyl]-2,2′-bipyridyl	32.09	1.38	612	$C_{28}H_{26}Br_2N_2O_4$
18	5,15-Bis(3-methoxyphe nyl)-10-phenyl-20-propylporphyrin	33.25	1.54	640	C43H36N4O2
19	9,12-Octadecadienoic acid, methyl ester, (E,E)- (CAS)	33.99	7.15	294	$C_{19}H_{34}O_2$
20	17-Pentatriacontene (CAS)	34.07	2.19	490	$C_{35}H_{70}$
21	6,6′,7,7′-Tetramethoxy5,5′-diisopropyl-8-bro mo-3,3′-bis(bromomethyl)dinaphtho [2,1-b:2′,1′-d]furan	35.40	1.62	734	$C_{32}H_{33}Br_3O_5$
22	(2"S,Sa,2‴S)-1,1-Dihy droxy-3,3-bis[2-hydroxy -1-propyl]-2,2′,4,4′,6,6′-hexamethoxy-5,5′-naphthalene	39.48	2.17	582	$C_{32}H_{38}O_{10}$
23	Ethyl 2-chloro-7-methoxy-5- methyl-1,4-naphthoqui none-6-carboxylate	40.94	1.37	308	$C_{15}H_{13}ClO_5$
24	36,37,38-Trimethoxy-5, 10,15-trimethyl-22,25, 30,33-tetraoxa-1,19-dia zapentacyclo[17.8.8.1(3,7).1(8,12).1(13,17)]octatriaconta-3,5,7(36)nonane	44.84	1.57	648	$C_{38}H_{52}N_2O_7$
25	2-(4-Pyridyl)-8-bromon aphth[1,2-*d*]oxazole	45.00	1.36	324	$C_{16}H_9BrN_2O$
26	tetraphenylporphyrinatodibromotitanium(IV)	45.30	1.71	818	$C_{44}H_{28}Br_2N_4Ti$
27	2-Dichloromethylene-1 -(2,4,6-tri-*t*-butylpheny l)-3-(2,2-diphenylmethenylene)-1-phosphirane	45.51	1.69	548	$C_{34}H_{39}Cl_2P$
28	2,2-Bis[4-[[4-chloro-6-(3-ethynylphenoxy)-1,3,5 -triazin-2-yl]oxy]pheny l]propane	45.70	2.69	686	$C_{37}H_{24}Cl_2N_6O_4$
29	5,16-Dibromo-6,15-dit hio-8,10,10,11,11,13-hexachloropentacyclo[10. 6.1.1(2,9).0 (3,7).0(14,1 8)]octadeca-dodecaene	45.95	1.63	658	$C_{18}H_{10}Br_2Cl_6S_2$
30	1,4-Di-hept-1-ynyl-2,3, 5,6-tetrakis(trimethylsil ylethynyl)benzene	46.03	2.32	650	$C_{40}H_{58}Si_4$
31	2-Methoxy-3-nitro-5,10,15,20-tetraphenyl-2,3-dihydroporphyrin	47.68	2.00	689	$C_{45}H_{31}N_5O_3$
32	5"-(1,1-Dimethylethyl) −2,2′,2″,2‴,2""-pentam ethoxy-[1,1':3′,1":3″,1‴:3‴.1""-quinquephenyl] −3,3""-dicarboxylic acid	47.88	2.08	676	$C_{41}H_{40}O_9$
33	Dimethyl 2,anti-4,anti-9,12,anti14-pentabromodecacyc lo[9.9.0.0(1,8).0(2,12). 0 (6,10).0(11,18)0(13,1 7).0(16,20)] icosane-*syn*-4,syn-9-dicarboxylate	48.17	1.79	770	$C_{24}H_{23}Br_5O_4$
34	2,4-bis(2-chloroethyl)- 8-hydroxymethyl)-6,7-b is[2-(methoxycarbonyl) ethyl]-1,3,5-trimethylporphyrin	49.51	1.56	678	$C_{36}H_{40}Cl_2N_4O_5$
35	2,2-Bis[4-[[4-chloro-6-(3-ethynylphenoxy)-1,3,5 -triazin-2-yl]oxy]pheny l]propane	49.64	1.80	686	$C_{37}H_{24}Cl_2N_6O_4$
36	4-(Pyrrolin-2′-ylidene)- isoquinoline	49.97	1.78	196	$C_{13}H_{12}N_2$
37	1,4-Di-hept-1-ynyl-2,3, 5,6-tetrakis(trimethylsil ylethynyl)benzene	50.52	3.19	650	$C_{40}H_{58}Si_4$
38	*N,N′*-Dicyclohexyl-1,7- dipyrrolidinylperylene-3,4:9,10-tetracarboxylic acid bisimide	51.21	1.51	692	$C_{44}H_{44}N_4O_4$
39	(2,2-Dibenzyloxy-3-nit ro-5,10,15,20-tetraphen yl-2,3-dihydroporphyrinato)copper (II)	51.86	1.37	901	$C_{58}H_{40}CuN_5O_2$
40	2,5-Dibromo-1,4-di-*n*-h exadecylbenzene	52.84	1.46	682	$C_{38}H_{68}Br_2$
41	(5,10,15,20-tetraphenyl[2-(2)H1]prophyrinato)zinc(II)	52.99	1.60	676	$C_{44}H_{28}Br_2N_4Zn$
42	Dichloro(5,10,15,20-tet raphenylporphyrinato)vanadium	53.04	2.14	733	$C_{44}H_{28}Cl_2N_4V$
43	Bis[(2,4,6-Tri-*tert*-butyl phenyl)amino]phenylchlorosilane	53.15	2.01	660	$C_{42}H_{65}ClN_2Si$
44	3,5-cyclo-6-methoxy-à(iodotetradecyl)pregnanoic acid ethyl ester	53.28	1.40	696	$C_{38}H_{65}IO_3$
45	(2-Formamido-3-nitro5,10,15,20-tetraphenyl porphyrinato)copper(II)	53.44	1.93	763	$C_{45}H_{28}CuN_6O_3$
46	5-(2-Bromoethylidene) -4-*t*-butoxyfuran-2(5H)-one	54.13	1.76	260	$C_{10}H_{13}BrO_3$
47	(2-hydroxy-5,10,15,20-t etraphenylporphinato)zinc(II)	54.61	1.45	692	$C_{44}H_{28}N_4OZn$

3.12. Optimization of bioremoval process parameters to enhance bioremoval efficiency of heavy metals from the real refinery wastewater by the dead biomass of JAZ-20

Given the substantial volume of water utilized in petrol refining operations, the petroleum refining industry increasingly demands

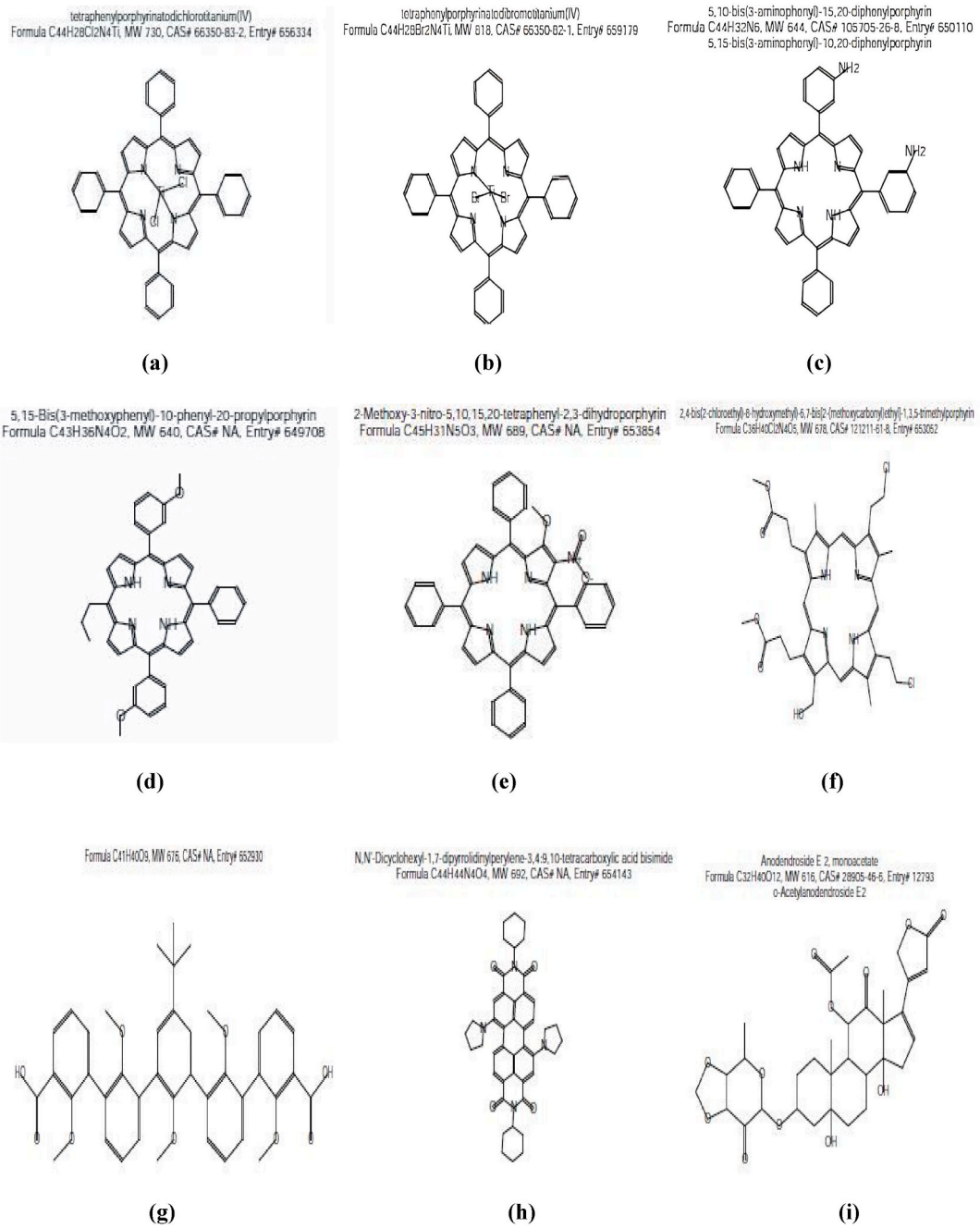

Fig. 8. Chemical structure of some bioactive volatile compounds detected in the ethyl acetate extract of JAZ-20 fungus.

more efficient management and reuse of wastewater. This necessitates the exploration of novel industrial wastewater treatment technologies [69]. In this context, harnessing indigenous mycobiomes from industrial effluents and optimizing bioremoval process parameters emerge as crucial support processes for safe refinery operation [19,20]. Data presented in Table 8 revealed that the dead biomass of JAZ-20 exhibits superior bioremoval capacity for the nine heavy metals studied, extracted from refinery wastewater under various operational conditions.

3.12.1. Optimization of contact time

The effectiveness of removing heavy metals from the environment through bioremoval relies on the duration of contact between biomass and contaminants [1]. Therefore, the dead biomass of the JAZ-20 fungus was combined with actual refinery wastewater

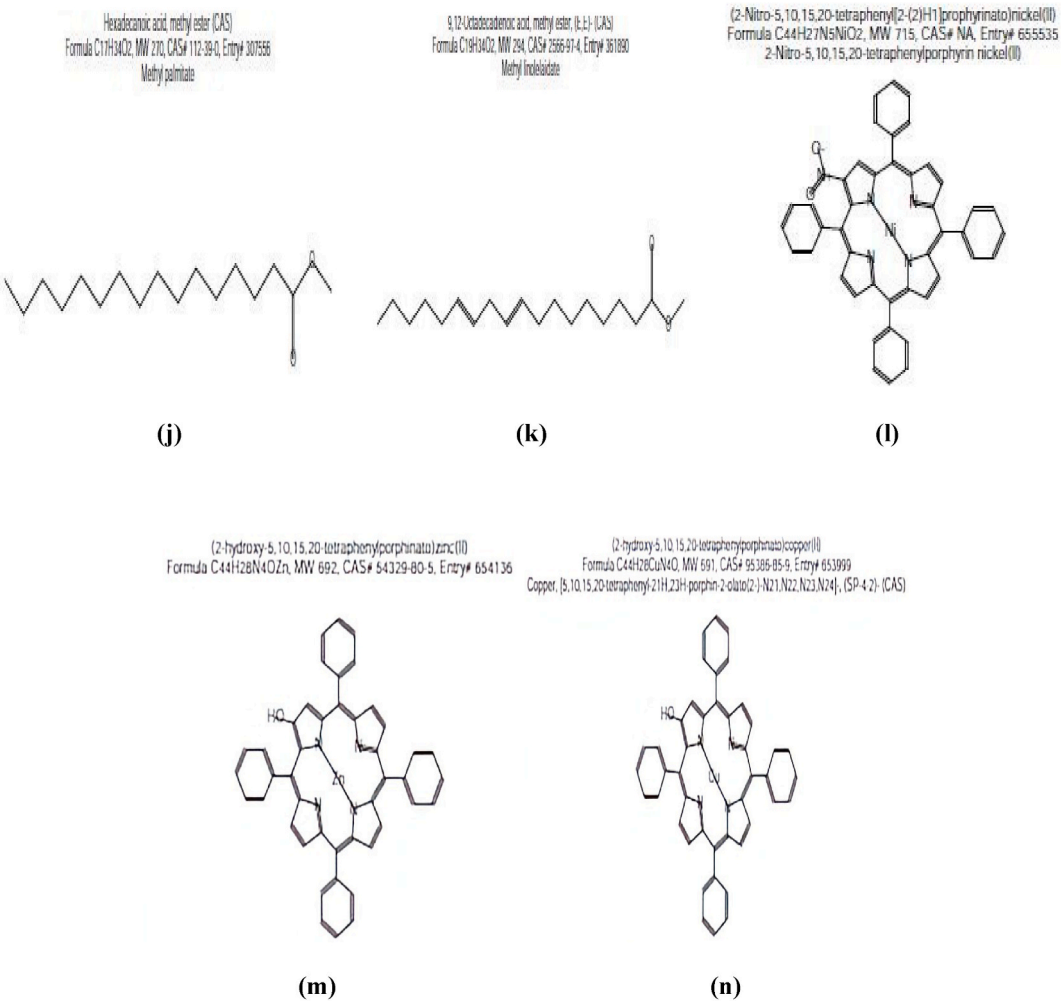

Fig. 8. (*continued*).

containing these heavy metals, as outlined previously, for varying periods of 10, 20, 30, 60, 120, and 180 min to determine the optimal contact time for the bioremoval process. Table 8 reveals that complete bioremoval for Fe^{3+}, Pb^{2+}, Hg^{2+}, and Al^{3+} (100 %) were attained after 60 min of contact time with the dead biomass of JAZ-20, whereas full removal of Cd^{2+}, Mn^{2+}, and Ni^{3+} (100 %) occurred rapidly following 30 min of contact time. Conversely, extended contact times of 120 and 180 min were necessary for JAZ-20 biomass to achieve 100.0 and 67.09 % bioremoval of Cr^{6+} and As^{3+}, respectively. Consistent with our findings, Zareh et al. observed that prolonged incubation of *Aspergillus niger* with Zn and Ag resulted in decreased binding of these metals to the fungal biomass. This phenomenon could be attributed to the saturation of free binding active sites on the outer surface over time, leading to biosorption occurring primarily on the outer surface rather than the inner surface [70].

3.12.2. Optimization of the JAZ-20 biomass dosage

As shown in Table 8, increasing the biosorbent concentration from 0.05 to 0.1, 0.2, 0.5 and 1.0 % resulted in extensive increase in the bioremoval of Fe^{3+} (RE = 15.42 ± 1.25 %, 34.1 ± 1.69 %, 63.95 ± 2.51 %, 100.0 ± 3.14 % and 100.0 ± 2.97 %), Al^{3+} (RE = 30.5 ± 1.69 %, 53.9 ± 2.27 %, 85.13 ± 2.7 %, 100.0 ± 2.96 % and 100.0 ± 2.96 %), Cd^{2+} (18.3 ± 0.73 %, 42.19 ± 2.0 %, 84.2 ± 2.4 %, 100.0 ± 2.5 % and 100.0 ± 2.52 %), Mn^{2+} (24.5 ± 0.81 %, 59.13 ± 1.3 %, 80.13 ± 2.5 %, 100.0 ± 1.96 %, and 100.0 ± 2.0 %), Ni^{2+} (30.5 ± 1.11 %, 60.0 ± 1.25 %, 85.13 ± 1.7 %, 100.0 ± 2.19 % and 100.0 ± 2.19 %), and Cr^{6+} (34.65 ± 1.19 %, 70.13 ± 1.5 %, 90.0 ± 1.84 %, 100.0 ± 1.96 % and 100.0 ± 1.94 %). Moreover, 100.0 % removal in Pb^{2+} and Hg^{2+} were achieved at lower biomass concentrations equal to 0.2 % biomass. The reduction efficiencies obtained were RE = 34.5 ± 1.7 %, 69.88 ± 2.19 %, 100.0 ± 2.98 %, 100.0 ± 2.83 %, and 100.0 ± 2.83 % for Pb^{2+} and RE = 38.44 ± 1.45 %, 71.56 ± 2.3 %, 100.0 ± 2.91 %, 100.0 ± 2.96 % and 100.0 ± 3.08 % for Hg^{2+} (Table 8). Interestingly, removal of As^{3+} by 76.24 % needs higher concentration of biomass equal to 1.0 %. Conversely, there might be a lower affinity between the JAZ-20 biomass and As^{3+}, as indicated by needing for a higher biomass amount (1.0 %) to adsorb 76.24 % of As^{3+} from effluents containing a mixture of heavy metals (Table 8). In contrast, lower reduction equal to 15.42 ± 1.25 % for Fe^{3+}, 34.5 ± 1.7 % for Pb^{2+}, 38.44 ± 1.45 % for Hg^{2+}, 30.5 ± 1.19 % for Al^{3+}, 18.3 ± 0.73 % for Cd^{2+}, 24.5 ±

Table 7
Characterization the metal ions in the petroleum refining wastewater at Jazan city.

Parameter	Concentration of heavy metals (mg/L)		
	Petroleum refining wastewater	Allowable limit guidelines (water quality)	
		WHO (2011)	USEPA(2009)
Sodium (Na^{+})	3570.48 ± 10.42	200	20.20
Potassium (K^{+})	139.20 ± 1.12	10	–
Magnesium (Mg^{2+})	359.80 ± 2.57	150	–
Calcium (Ca^{2+})	560.93 ± 3.18	75	–
Aluminum (Al^{3+})	185.17 ± 1.40	–	0.05–0.2
Iron (Fe^{3+})	3015.68 ± 11.15	0.20	2.0
Manganese (Mn^{2+})	267.52 ± 2.40	0.5	0.1
Cupper (Cu^{2+})	19.92 ± 0.33	2	1.3
Zinc (Zn^{2+})	35.31 ± 0.96	5.00	5.0–7.40
Lead (Pb^{2+})	41.15 ± 0.38	0.01	0.015
Cobalt (Co^{2+})	224.30 ± 2.51	–	–
Nickel (Ni^{2+})	27.46 ± 0.40	0.070	0.61
Arsenic (As^{3+})	3.13 ± 0.13	0.01	–
Cadmium (Cd^{2+})	2.27 ± 0.07	0.003	0.005
Chromium (Cr^{6+})	7.90 ± 0.19	0.05	0.1
Barium (Ba^{2+})	166.37 ± 1.31	0.7	1.0
Silver (Ag^{+})	3.00 ± 0.15	–	–
Mercury (Hg^{2+})	0.130 ± 0.00	0.001	0.004
pH	8.0 ± 0.02	–	–
BOD (mg/L)	175.38 ± 3.00	–	–
COD (mg/L)	453.70 ± 4.58	–	–
TSS (mg/L)	221.95 ± 3.61	–	–
TDS (mg/L)	516.12 ± 4.10	250	–
NH3 (mg/L)	9.75 ± 1.07	–	–
Phenols (mg/L)	11.68 ± 1.22	–	4
Sulfides (mg/L)	16.94 ± 1.40	–	–
Oil and Grease (mg/L)	203.39 ± 3.90	–	–

0.81 % for Mn^{2+}, 30.5 ± 1.11 % for Ni^{2+}, 34.65 ± 1.19 % for Cr^{6+} and 11.42 ± 0.38 % for As^{3+} when the biomass decreased from the optimum dosages to 0.05 % as outlined in Table 8. Alhamd et al. proved that he increases in the bioremoval capacity of heavy metals can be attributed to the fixed amount of fungal biosorbents, which enhances the available number of binding sites and the bioremoval surface area of fungal biomass from *Trichoderma viride*, *A. flavus*, *A. niger, A. tamari*, *P. brevicompactum*, *P. citrinum* and *Penicillium* sp. 104 for metal bioremoval [71].

3.12.3. Optimization of pH

Various pH values ranging from 2 to 6 were employed in the bioremoval processes to investigate their impact on the biosorption of JAZ-20 biomass toward Fe^{3+}, Pb^{2+}, Hg^{2+}, Al^{3+}, Mn^{2+}, Ni^{2+}, Cr^{6+}, Cd^{2+} and As^{3+}. The results presented in Table 8 indicated that the highest bioremoval efficiency (100.0 %) of Fe^{3+}, Pb^{2+} and Al^{3+} from refinery wastewater was achieved at pH 4.0 to 5.0, while pH 5.0 was optimal for complete removing of Hg^{2+}, Cd^{2+} and Ni^{2+} (Table 8). Moreover, reduction in the effluent contents of Cr^{6+} and As^{3+} reaching 100.0 ± 2.2 % and 88.24 ± 1.75 %, respectively upon contact with the fungal biomass at pH 6.0 but Mn^{2+} was completely removed from the wastewater at pH 4.0 (Table 8). pH exerts a notable influence on the physiology and metabolism of fungi, leading to indirect effects on metal accumulation. Fungal growth, enzyme activity, and various cellular processes are intricately linked to pH levels. Any pH-induced alterations in these factors can influence the ability of fungi to accumulate and tolerate toxic metals [71]. Consistent with our findings, El-Gendy et al., demonstrated that the effectiveness of dead biomass from *Drechslera hawaiiensis* in removing Cd^{2+}, Cu^{2+}, and Pb^{2+} from aqueous solutions was optimal within the pH range of 6–7.

3.12.4. Optimization of temperature

Furthermore, the operational temperature ranges of 35–40 °C facilitated the best bioremoval of Al^{3+}, Ni^{2} and As^{3+} from refinery effluents to reach 100.0, 100.0 and 91.65 % while bioremoval rates decreased as the temperature increased until reaching 55.36 ± 2.22 %, 42.0 ± 2.26 % and 37.47 ± 0.7 %, respectively at 60 °C (Table 8). The bioremoval of Hg^{2+} and Mn^{2+} showed no sensitivity with increasing temperature from 35 up to 50 °C (100.0 % bioremoval) and hence the bioremoval process inhibited by 14.83 % and 9.88 %, respectively when the process temperature increased to 60 °C (Table 8) but the removal process for Fe^{3+}, Pb^{2+}, Cd^{2+} and Cr^{6+} was optimal at temperature ranged from 35 up to 45 °C and then the removal efficiency decreased to (62.48 ± 2.35 % and 40.7 ± 1.42 %), (98.0 ± 3.25 % and 72.15 ± 2.73 %), (78.9 ± 2.15 % and 55.36 ± 2.22 %), and (80.32 ± 1.65 % and 72.8 ± 1.56 %) at 50 and 60 °C, respectively (Table 8). The bioremoval efficiency of Fe^{3+} and Co^{2+} using the biomass of *Aspergillus* sp. AHM69 increased by 25.27 and 19.81 %, respectively, as the process temperature rose from 40 °C to 45–55 °C. Similarly, the bioremoval of Fe^{3+} and Co^{2+} using the biomass of *Penicillium* sp. AHM96 increased from 51.7 to 79.15 % at 40 °C to 53.94 % and 90.34 % at 45 °C [4].

Table 8
Optimization of the process parameters for enhancing bioemoval efficiency (%) of the selected heavy metals from the real refinery wastewater by the dead biomass of fungus JAZ-20.

Parameter	Heavy metals adsorption (%)								
	Fe^{3+}	Pb^{2+}	Hg^{2+}	Al^{3+}	Cd^{2+}	Mn^{2+}	Ni^{2+}	Cr^{6+}	As^{3+}
Contact time ((h)									
10	17.60 ± 1.64	15.70 ± 1.27	53.90 ± 1.75	37.90 ± 1.46	50.14 ± 1.80	54.16 ± 0.98	44.35 ± 1.15	10.50 ± 0.42	9.08 ± 0.31
20	49.74 ± 2.15	40.16 ± 1.65	69.23 ± 1.88	63.00 ± 1.62	72.50 ± 1.74	80.00 ± 1.32	62.30 ± 1.70	34.61 ± 0.75	15.37 ± 0.55
30	75.17 ± 2.51	66.75 ± 2.00	90.00 ± 2.65	81.13 ± 1.69	100.00 ± 2.19	100.00 ± 1.70	100.00 ± 1.92	65.30 ± 1.29	32.62 ± 0.68
60	100.00 ± 2.90	100.00 ± 3.10	100.00 ± 2.82	100.00 ± 1.92	100.00 ± 2.10	100.00 ± 1.84	100.00 ± 1.92	92.49 ± 1.72	50.01 ± 0.90
120	90.44 ± 2.87	100.00 ± 3.11	100.00 ± 2.69	90.78 ± 1.87	95.78 ± 1.28	100.00 ± 1.91	97.13 ± 1.80	100.00 ± 2.13	55.36 ± 1.00
180	85.19 ± 2.29	94.21 ± 3.00	97.50 ± 2.02	89.63 ± 1.28	92.63 ± 0.87	99.63 ± 2.83	96.80 ± 1.72	100.00 ± 2.02	67.09 ± 1.30
Fungus biomass dose (%)									
0.05	15.42 ± 1.25	34.50 ± 1.70	38.44 ± 1.45	30.50 ± 1.19	18.30 ± 0.73	24.50 ± 0.81	30.50 ± 1.11	34.65 ± 1.19	11.42 + 0.38
0.1	34.10 ± 1.69	69.88 ± 2.19	71.56 ± 2.30	53.90 ± 2.27	42.19 ± 2.00	59.13 ± 1.30	60.00 ± 1.25	70.13 ± 1.50	29.13 ± 0.62
0.2	63.95 ± 2.51	100.00 ± 2.98	100.00 ± 2.91	85.13 ± 2.70	84.20 ± 2.40	80.13 ± 2.50	85.13 ± 1.70	90.00 ± 1.84	50.80 ± 0.98
0.5	100.00 ± 3.14	100.00 ± 2.83	100.00 ± 2.96	100.00 ± 2.96	100.00 ± 2.50	100.00 ± 1.96	100.00 ± 2.19	100.00 ± 1.96	69.12 ± 1.43
1.0	100.00 ± 2.97	100.00 ± 2.83	100.00 ± 3.08	100.00 ± 0.69	100.00 ± 2.52	100.00 ± 2.00	100.00 ± 2.19	100.00 ± 1.94	76. 24 ± 1.55
pH									
2	40.18 ± 1.53	46.70 ± 1.45	28.00 ± 1.25	39.51 ± 1.37	26.86 ± 0.99	39.51 ± 1.37	20.93 ± 1.00	50.31 ± 1.35	42.83 ± 0.87
3	94.16 ± 2.85	63.12 ± 1.84	69.57 ± 2.43	66.13 ± 3.26	40.15 ± 0.83	70.42 ± 1.88	48.56 ± 1.95	80.49 ± 1.70	74.91 ± 1.64
4	100.00 ± 3.00	100.00 ± 2.92	80.00 ± 3.21	100.00 ± 3.58	59.00 ± 1.76	100.00 ± 2.50	60.27 ± 1.80	74.02 ± 1.56	76.30 ± 1.52
5	100.00 ± 3.00	100.00 ± 2.90	100.00 ± 3.13	100.00 ± 3.53	100.00 ± 2.11	60.65 ± 1.95	100.00 ± 2.70	89.88 ± 1.20	80.20 ± 1.69
6	85.66 ± 2.70	75.00 ± 2.47	70.00 ± 2.19	90.27 ± 1.71	79.47 ± 1.86	51.38 ± 1.71	66.13 ± 2.16	100.00 ± 2.20	88.24 ± 1.75
Temperature (°C)									
35	100.00 ± 2.76	100.00 ± 2.00	100.00 ± 2.90	100.00 ± 3.10	100.00 ± 3.10	100.00 ± 2.61	100.00 ± 2.80	100.00 ± 1.93	88.22 ± 1.75
40	100.00 ± 2.78	100.00 ± 3.12	100.00 ± 2.92	100.00 ± 3.01	100.00 ± 3.01	100.00 ± 2.63	100.00 ± 2.96	100.00 ± 1.89	91.65 ± 1.88
45	100.00 ± 2.70	100.00 ± 3.19	100.00 ± 2.90	85.00 ± 2.80	100.00 ± 3.00	100.00 ± 2.72	75.12 ± 2.55	100.00 ± 1.90	79.50 ± 1.67
50	62.48 ± 2.35	98.00 ± 3.25	100.00 ± 2.85	70.12 ± 2.47	78.90 ± 2.15	100.00 ± 2.75	60.80 ± 2.39	80.32 ± 1.65	63.28 ± 1.53
60	40.70 ± 1.42	72.15 ± 2.73	85.17 ± 2.60	55.36 ± 2.22	55.36 ± 2.22	90.12 ± 2.46	42.00 ± 2.26	72.80 ± 1.56	37.47 ± 0.70
Agitation speed (rpm)									
100	71.25 ± 2.11	77.69 ± 2.34	88.21 ± 2.51	90.39 ± 3.43	91.50 ± 2.79	54.16 ± 1.62	69.84 ± 1.91	78.61 ± 1.46	61.50 ± 1.45
125	100.00 ± 2.59	100.00 ± 2.55	100.00 ± 2.85	100.00 ± 3.01	100.00 ± 2.94	100.00 ± 2.68	100.00 ± 2.96	100.00 ± 1.96	91.59 ± 1.97
150	90.23 ± 2.38	91.30 ± 2.67	94.51 ± 2.56	91.56 ± 2.93	90.94 ± 2.86	72.15 ± 1.97	89.50 ± 2.85	74.32 ± 1.65	93.65 ± 1.84
200	63.45 ± 2.00	61.6 ± 2.30	62.86 ± 2.03	89.50 ± 2.74	79.22 ± 2.39	60.86 ± 1.86	68.21 ± 1.83	71.25 ± 1.70	75.1 ± 1.65
250	40. 21 ± 1.75	47.46 ± 1.62	40.96 ± 1.61	83.43 ± 2.46	63.51 ± 2.14	40.30 ± 1.35	50.19 ± 1.69	69.57 ± 1.60	54.18 ± 1.28

3.12.5. Optimization of agitated rate

The stirring rates had a notable impact on the effectiveness of the bioremoval process for numerous heavy metals, as recorded in Table 8. Removal percentages were recorded at 71.25 ± 2.11, 100.0 ± 2.59, 90.23 ± 2.38, 63.45 ± 2.0, 40. 21 ± 1.75 for Fe^{3+}; 77.69 ± 2.34, 100.0 ± 2.55, 91.3 ± 2.67, 61.6 ± 2.3 and 47.46 ± 1.62 for Pb^{2+}; 88.21 ± 2.51, 100.0 ± 2.85, 94.51 ± 2.56, 62.86 ± 2 0.03 and 40.96 ± 1.61 for Hg^{2+}; 90.39 ± 3.43, 100.0 ± 3.01, 91.56 ± 2.93, 89.5 ± 2.74 and 83.43 ± 2.46 for Al^{3+}; 91.5 ± 2.79, 100.0 ± 2.94, 90.94 ± 2.86, 79.22 ± 2.39, and 63.51 ± 2.14 for Mn^{2+} when agitated at 100, 125, 150, 200 and 250 rpm, respectively (Table 8).

Moreover, reduction percentages equal to 54.16 ± 1.62, 100.0 ± 2.68, 72.15 ± 1.97, 60.86 ± 1.86, and 40.3 ± 1.35 for Ni^{2+}; 69.84 ± 1.91, 100.0 ± 2.96, 89.5 ± 2.85, 68.21 ± 1.83 and 50.19 ± 1.69 for Cr^{6+}; 78.61 ± 1.46, 100.0 ± 1.96, 74.32 ± 1.65, 71.25 ± 1.7 and 69.57 ± 1.6 for Cd^{2+} and 61.5 ± 1.45, 91.59 ± 1.97, 93.65 ± 1.84, 75.1 ± 1.65, 54.18 ± 1.28 for As^{3+} were recorded after agitated the JAZ-20 biomass with the petroleum refining wastewater under condition optimized earlier at agitation rate 100, 125, 150, 200 and 250 rpm, respectively (Table 8). Our findings are somewhat consistent with those of Ho et al. they emphasized that the presence of heavy metals in refinery effluents can pose significant risks to both human health and the environment. They also highlighted the limitations of conventional heavy metal removal methods, thus advocating for the exploration of alternative treatments. They mentioned that bio-adsorption of heavy metals using fungi has garnered considerable interest due to its ability to achieve effective removal rates [72]. For instance, removal rates of 80 % for iron, 99 % for zinc, 94 % for lead, 99 % for nickel, 93 % for chromium and 96 % for cadmium from refinery effluents using the living white rot fungus *Pleurotus ostreatus*, under conditions of pH 7.6, temperature of 26.8 °C and prolonged contact time [72].

4. Conclusions

The Economic City in the Saudi Arabia hosts numerous industries, particularly in the energy and manufacturing sectors. It is evident that hydrocarbons and heavy metals present in their effluents constitute significant pollutants in the environment. The aim of this research was to isolate, identify, and evaluate the bioremoval capacity of indigenous fungal mycobiome sourced from petroleum refining wastewater collected from the refinery industry in the Jazan region, Saudi Arabia toward crude oil, hydrocarbons, pharmaceuticals, agrochemicals and heavy metals pollution from the refining effluents. Thirty-two fungal isolates were obtained from petroleum refining effluents, characterized and categorized into 5 groups; *Fusarium* (10 isolates), *Verticillium* (7 isolates), *Purpureocillium* (5 isolates), *Clavispora* (4 isolates) and *Scedosporium* (6 isolates). The study examined the potential distribution of multidrug-resistant fungal strains against various classes of antifungal antibiotics, including azoles, echinocandins, and polyenes, with the aim of identifying and eliminating MDR strains from environmental applications. Furthermore, the most hyperactive biosorbent strain, exhibiting and demonstrating potent removal efficiencies for crude oil, hydrocarbons, heavy metals, and other pollutants from aqueous solutions along with its minimal resistance to fungal antibiotics was selected for phylogenetic, VOC metabolic profile and optimization of process parameters for the adsorption of heavy metals from real refinery wastewater. Among the obtained mycobiome the JAZ-20 fungus proved to be one of the promising remediation technologies that can give efficient inexpensive and sustainable approach for the large-scale wastewater remediation. Based on morphological, biochemical phylogenetic analysis JAZ-20 fungus was identified as *S. apiospermum* JAZ-20, which isolated for the first time from industrial effluents in Saudi Arabia. Methane chloride extract of *S. apiospermum* JAZ-20 gave anti-proliferative activity against 5 types of human normal cells and 3 types of cancerous cells. The volatile compounds profile of the methylene chloride extract of *S. apiospermum* was determined by GC–MS analysis, which proved 47 compounds with varied biological applications. The parameters including contact time, biomass dosages, pH, temperature and agitation rate of heavy metals removal process parameters were optimized.

Funding statement

This research was funded by Researchers Supporting Project number (RSP2024R364), King Saud University, Riyadh, Saudi Arabia.

Data availability statement

Data included in article/supp. Material/referenced in article.

Additional information

No additional information is available for this paper.

CRediT authorship contribution statement

Fuad Ameen: Writing – review & editing, Writing – original draft, Visualization, Validation, Investigation, Data curation, Conceptualization. **Mohammad J. Alsarraf:** Validation, Investigation, Data curation, Conceptualization. **Tarad Abalkhail:** Writing – review & editing, Writing – original draft, Visualization, Validation, Investigation, Funding acquisition, Data curation, Conceptualization. **Steven L. Stephenson:** Writing – review & editing, Writing – original draft, Investigation, Conceptualization.

Declaration of competing interest

The authors declare that they have no known competing financial interests or personal relationships that could have appeared to influence the work reported in this paper.

Acknowledgments

This research was funded by Researchers Supporting Project number (RSP2024R364), King Saud University, Riyadh, Saudi Arabia.

References

[1] M.M.A. El-Gendy, A.M.A. El-Bondkly, Evaluation and enhancement of heavy metals bioremediation in aqueous solutions by *Nocardiopsis* sp. MORSY1948, and *Nocardia* sp. MORSY2014, Braz. J. Microbiol. 7 (3) (2016) 571–586.

[2] G.E. Hejazy, N.A. Soliman, S. Farag, E.R. El-Helow, H.Y. Hassan, Y.R. Abdel-Fattah, Isolation and characterization of *Candida tropicalis* B: a promising yeast strain for biodegradation of petroleum oil in marine environments, Microb. Cell Factories 23 (1) (2024) 20, https://doi.org/10.1186/s12934-023-02292-y, 13.

[3] C. Medina-Armijo, D. Isola, J. Illa, A. Puerta, M. Viñas, F.X. Prenafeta-Boldú, The Metallotolerance and biosorption of As(V) and Cr(VI) by black fungi, J. Fungi (Basel) 10 (1) (2024) 47, https://doi.org/10.3390/jof10010047, 5.

[4] A.M.A. El-Bondkly, M.M.A.A. El-Gendy, Bioremoval of some heavy metals from aqueous solutions by two different indigenous fungi *Aspergillus sp.* AHM69 and *Penicillium sp.* AHM96 isolated from petroleum refining wastewater, Heliyon 8 (7) (2022) e09854, https://doi.org/10.1016/j.heliyon.2022.e09854, 2.

[5] S.H. Chen, S.L. Ng, L.C. Yuen, A.S.Y. Ting, A novel study based on adaptive metal tolerance behavior in fungi and SEM-EDX analysis, J. Hazard Mater. 15 (334) (2017) 132–141, https://doi.org/10.1016/j.jhazmat.2017.04.004.

[6] A. Hassan, A. Periathamby, A. Ahmed, O. Innocent, F.S. Hamid, Effective bioremediation of heavy metal–contaminated landfill soil through bioaugmentation using consortia of fungi, J. Soils Sediments 20 (2020) 66–80.

[7] M. Elizondo-Zertuche, R. Treviño-Rangel, E. Robledo-Leal, C.E. Luna-Rodríguez, M.L. Martínez-Fierro, I.P. Rodríguez-Sánchez, G.M. González, Molecular identification and in vitro antifungal susceptibility of *Scedosporium* complex isolates from high-human-activity sites in Mexico, Mycologia 109 (6) (2017) 874–881, https://doi.org/10.1080/00275514.2017.

[8] A.A. Al-Sheikh, A. Albarrak, O. Dafalla, S. Noureldin, M. Waheedeldeen, K. Shrwani, et al., The use of nested-PCR to detect the presence of *Plasmodium* in *Anopheles arabiensis* in Jazan region, Saudi Arabia, J. Egypt. Soc. Parasitol. 47 (2017) 151–158.

[9] StG. Geraverage, R. Scedosporium Summerbell, Identifying Filamentous Fungi, second ed., Blackwell Science, Belmont, 1996.

[10] S. Giraud, J.-P. Bouchara, *Scedosporium apiospermum* complex: Diagnosis and species identification, Curr. Fungal Infect. Rep. 8 (2014) 211–219.

[11] Larone, D.H. Medically Important Fungi: A Guide to Identification. third ed., American Society for Microbiology.

[12] A. Puszkarewicz, J. Kaleta, The efficiency of the removal of naphthalene from aqueous solutions by different adsorbents, Int. J. Environ. Res. Publ. Health 17 (2020) 5969, https://doi.org/10.3390/ijerph17165969.

[13] American Public Health Association (APHA), Standard Methods for the Examination of Water and Wastewater (SMWW), 23rd ed., 2018. Washington, DC, USA.

[14] S. Zafar, F. Aqil, I. Ahmad, Metal tolerance and biosorption potential of filamentous fungi isolated from metal contaminated agricultural soil, Biores.Technol. 98 (2007) 2557–2561.

[15] Clinical Laboratory Standards Institute (CLSI), CLSI Reference Method for Broth Dilution Antifungal Susceptibility Testing of Filamentous Fungi, 3 rd edition, 2017. CLSI Standards M38. Wayne, Pa.

[16] M.M.A. El-Gendy, A.M.A. El-Bondkly, S.M.M. Yahya, Production and evaluation of antimycotic and antihepatitis C virus potential of fusant MERV6270 derived from mangrove endophytic fungi using novel substrates of agroindustrial wastes, Appl. Biochem. Biotechnol. 174 (2014) 2674–2701, https://doi.org/10.1007/s12010-014-1218-2.

[17] A.M.A. El-Bondkly, Molecular identification using ITS sequences and genome shuffling to improve 2- deoxyglucose tolerance and xylanase activity of marine-derived fungus, *Aspergillus sp*, NRCF5. Appl. Biochem. Biotechnol. 167 (2012) 2160–2173, https://doi.org/10.1007/s12010-012-9763-z.

[18] T.J. White, T. Bruns, S. Lee, J.W. Taylor, Amplification and direct sequencing of fungal ribosomal RNA genes for phylogenetics, in: M.A. Innis, D.H. Gelfand, J. J. Sninsky, T.J. White (Eds.), PCR Protocols: a Guide to Methods and Applications, Academic, New York, 1990, pp. 315–322.

[19] M.M.A.A. El-Gendy, S.M. Abdel-Moniem, N.S. Ammar, A.M.A. El-Bondkly, Bioremoval of heavy metals from aqueous solution using dead biomass of indigenous fungi derived from fertilizer industry effluents: isotherm models evaluation and batch optimization, Biometals 36 (6) (2023) 1307–1329.

[20] M.M.A.A. El-Gendy, S.M. Abdel-Moniem, N.S. Ammar, A.M.A. El-Bondkly, Multimetal bioremediation from aqueous solution using dead biomass of *Mucor sp.* NRCC6 derived from detergent manufacturing effluent, J. Appl. Genet. 64 (3) (2023) 569–590, https://doi.org/10.1007/s13353-023-00765-9.

[21] S. Kumar, G. Stecher, M. Li, C. Knyaz, K. Tamura, X. Mega, Molecular evolutionary genetics analysis across computing platforms, Mol. Biol. Evol. 35 (2018) 1547–1549.

[22] K. Tamura, G. Stecher, S. Kumar, Mega 11: molecular evolutionary genetics analysis version 11, Mol. Biol. Evol. 38 (7) (2021) 3022–3027, https://doi.org/10.1093/molbev/msab120.

[23] T. Mosmann, Rapid colorimetric assay for cellular growth and survival: application to proliferation and cytotoxicity assays, J. Immunol. Methods 65 (1983) 55–63.

[24] T.H. Anderson, K.H. Domsch, W. Gams, Compendium of Soil Fungi, Lubrecht & Cramer Ltd, 1995, 3-9803083-8-3.

[25] K.H. Domsch, W. Gams, T.H. Anderson, Compendium of Soil Fungi, second ed., Lubrecht & Cramer Ltd, 2007, p. 322, 978-3-9803083-8-0.

[26] R.A. Samson, Paecilomyces and some allied hyphomycetes, Stud. Mycol. 6 (1974) 58.

[27] T. Kitisin, S. Ampawong, W. Muangkaew, P. Sukphopetch, Phenomic profiling of a novel sibling species within the *Scedosporium* complex in Thailand, BMC Microbiol. 21 (2021) 42, https://doi.org/10.1186/s12866-021-02105-5.

[28] A.N. Alabssawy, A.H. Hashem, Bioremediation of hazardous heavy metals by marine microorganisms: a recent review, Arch. Microbiol. 206 (3) (2024) 103, https://doi.org/10.1007/s00203-023-03793-5.

[29] K.E. Hammel, Mechanisms for polycyclic aromatic hydrocarbon degradation by ligninolytic fungi, Environ. Health Perspect. 103 (Suppl 5) (1995) 41–43, https://doi.org/10.1289/ehp.95103s441.

[30] N. Agrawal, P. Verma, S.K. Shahi, Degradation of polycyclic aromatic hydrocarbons (phenanthrene and pyrene) by the ligninolytic fungi *Ganoderma lucidum* isolated from the hardwood stump, Bioresour. Bioprocess. 5 (2018) 11, https://doi.org/10.1186/s40643-018-0197-5.

[31] A.D. Chane, Z. Košnář, T. Hřebečková, M. Jozífek, P. Doležal, P. Tlustoš, Persistent polycyclic aromatic hydrocarbons removal from sewage sludge-amended soil through phytoremediation combined with solid-state ligninolytic fungal cultures, Fungal Biol. 128 (2) (2024) 1675–1683.

[32] X. Dai, J. Lv, S. Guo, W. Wei, Heavy oil biodegradation by mixed bacterial consortium of biosurfactant- producing and heavy oil-degrading bacteria, Pol. J. Environ. Stud. 30 (2020) 71–80, https://doi.org/10.15244/pjoes/120769.

[33] S. Varjani, A. Pandey, V.N. Upasani, Petroleum sludge polluted soil remediation: Integrated approach involving novel bacterial consortium and nutrient application, Sci. Total Environ. 763 (2021) 142934.

[34] B. Hernández-Sánchez, E. Santacruz-Juárez, F. Figueroa-Martínez, et al., A novel and efficient strategy for the biodegradation of di(2-ethylhexyl) phthalate by *Fusarium culmorum*, Appl. Microbiol. Biotechnol. 108 (2024) 94, https://doi.org/10.1007/s00253-023-12961-y.

[35] R. Zhuo, F. Fan, A comprehensive insight into the application of white rot fungi and their lignocellulolytic enzymes in the bioremoval of organic pollutants, Sci. Total Environ. 778 (2021) 146132.

[36] N.B. Krishnan, N.K. Velmurugan, P.S. Kumar, R. Gayathri, Fungal bioremediation approaches for the bioremoval of toxic pollutants: Mechanistic understanding for biorefinery applications, Chemosphere 350 (9) (2024) 141123, https://doi.org/10.1016/j.chemosphere.2024.141123.

[37] V. Kumar, S.K. Dwivedi, Mycoremediation of heavy metals: processes, mechanisms, and affecting factors, Environ. Sci. Pollut. Res. 28 (2021) 10375–10412, https://doi.org/10.1007/s11356-020-11491-8.

[38] H. Desai, D. Patel, B. Joshi, Screening and characterization of heavy metal resistant fungi for its prospects in bioremediation of contaminated soil, Int. J. Curr. Microbiol. App. Sci. 5 (4) (2016) 652–658.

[39] A.S. Ayangbenro, O.O. Babalola, A new strategy for heavy metal polluted environments: a Review of microbial biosorbents, Int. J. Environ. Res. Publ. Health 14 (1) (2017) 94, https://doi.org/10.3390/ijerph14010094.

[40] W.A. Akinkunmi, A.A.S.A. Husaini, A. Zulkharnain, T.M. Guan, H.A. Roslan, Mechanism of biosorption of Pb (ii) and Cu (ii) ions using dead biomass of *Fusarium equiseti* strain UMAS and *Penicillium citrinum* strain, UMAS B2. J.O.B.I.M.B. 4 (2) (2016) 1–6.

[41] D. Kerfahi, M.C. Ogwu, D. Ariunzaya, A. Balt, D. Davaasuren, O. Enkhmandal, T. Purevsuren, A. Batbaatar, M. Tibbett, S. Undrakhbold, B. Boldgiv, J.M. Adams, Metal-tolerant fungal communities are delineated by high zinc, lead, and copper concentrations in metalliferous Gobi Desert soils, Microb. Ecol. 79 (2) (2020) 420–431, https://doi.org/10.1007/s00248-019-01405-8.

[42] C.L. Văcar, E. Covaci, S. Chakraborty, B. Li, D.C. Weindorf, T. Frențiu, M. Pârvu, D. Podar, Heavy metal-resistant filamentous fungi as potential mercury bioremediators, J. Fungi 7 (5) (2021) 386, https://doi.org/10.3390/jof7050386.

[43] P.V. Bramhachari, Understanding the Microbiome Interactions in Agriculture and the Environment, Springer Nature, 2022 9789811936968, 981193696X.

[44] L.T. Morales, L.N. González-García, M.C. Orozco, et al., The genomic study of an environmental isolate of *Scedosporium apiospermum* shows its metabolic potential to degrade hydrocarbons, Stand. in Genomic Sci. 12 (2017) 71, https://doi.org/10.1186/s40793-017-0287-6.

[45] C.L. Feng, J. Li, X. Li, K.L. Li, K. Luo, X.S. Liao, et al., Characterization and mechanism of lead and zinc biosorption by growing *Verticillium insectorum* J3, PLoS One 13 (2018) e0203859, https://doi.org/10.1371/journal.pone.0203859.

[46] E. Hoque, J. Fritscher, Multimetal bioremediation and biomining by a combination of new aquatic strains of *Mucor hiemalis*, Sci. Rep. 9 (2019) 10318, https://doi.org/10.1038/s41598-019-46560-7.

[47] S. Ghosh, I. Rusyn, O.V. Dmytruk, K.V. Dmytruk, H. Onyeaka, M. Gryzenhout, Y. Gafforov, Filamentous fungi for sustainable remediation of pharmaceutical compounds, heavy metal and oil hydrocarbons, Front. Bioeng. Biotechnol. 11 (2023) 1106973, https://doi.org/10.3389/fbioe.2023.1106973.

[48] N.P. Wiederhold, Antifungal resistance: current trends and future strategies to combat, Infect. Drug Resist. 10 (2017) 249–259, https://doi.org/10.2147/IDR.S124918.

[49] P.K. Dimitrios, Antifungal resistance: an emerging reality and a global challenge, J. Infect. Dis. 216 (2017) S431–S435.

[50] M.C. Arendrup, N. Friberg, M. Mares, G. Kahlmeter, J. Meletiadis, J. Guinea, How to interpret MICs of antifungal compounds according to the revised clinical breakpoints v. 10.0 European committee on antimicrobial susceptibility testing (EUCAST), Clin. Microbiol. Infection 26 (11) (2020) 1464–1472.

[51] D. Sanglard, Emerging threats in antifungal-resistant fungal pathogens, Front. Med. 3 (2016) 11, https://doi.org/10.3389/fmed.2016.00011.

[52] K.J. Cortez, E. Roilides, F. Quiroz-Telles, et al., Infections caused by *Scedosporium sp*, Clin. Microbiol. Rev. 21 (1) (2008) 157–197, https://doi.org/10.1128/CMR.00039-07.

[53] P. Munoz, M. Marin, P. Tornero, P.M. Rabadan, M. Rodrfguez-Creixens, E. Bouza, Successful outcome of *Scedosporium apiospermum* disseminated infection treated with voriconazole in a patient receiving corticosteroid therapy, Clin. Infect. Dis. 31 (2000) 1499–1501.

[54] F. Gilgado, J. Cano, J. Gené, D.A. Sutton, J. Guarro, Molecular and phenotypic data supporting distinct species statuses for *Scedosporium apiospermum* and *Pseudallescheria boydii* and the proposed new species *Scedosporium dehoogii*, J. Clin. Microbiol. 46 (2) (2008) 766–771, https://doi.org/10.1128/JCM.01122-07.

[55] M.F. Awad, F.S. El-Shenawy, M.M.A.A. El-Gendy, E.A.M. El-Bondkly, Purification, characterization, and anticancer and antioxidant activities of L-glutaminase from *Aspergillus versicolor* Faesay4, Int. Microbiol. 24 (2) (2021) 169–181.

[56] A.A.M. El-Bondkly, M.M.A.A. El-Gendy, A.M.A. El-Bondkly, Construction of efficient recombinant strain through genome shuffling in marine endophytic *Fusarium sp.* ALAA-20 for improvement lovastatin production using agro-industrial wastes, Arabian J. Sci. Eng. 46 (2021) 175–190, https://doi.org/10.1007/s13369-020-04925-5.

[57] M.M.A.A. El-Gendy, H.A.A. Al-Zahrani, A.M.A. El-Bondkly, Genome shuffling of mangrove endophytic *Aspergillus luchuensis* MERV10 for improving the cholesterol-lowering agent lovastatin under solid state fermentation, MYCOBIOLOGY 44 (3) (2016) 171–179, https://doi.org/10.5941/MYCO.2016.44.3.171.

[58] M.M.A.A. El-Gendy, S.H.M. Al-Zahrani, A.M.A. El-Bondkly, Construction of potent recombinant strain through intergeneric protoplast fusion in endophytic fungi for anticancerous enzymes production using rice straw, Appl. Biochem. Biotechnol. 183 (2017) 30–50, https://doi.org/10.1007/s12010-017-2429-0.

[59] M.M.A.A. El-Gendy, M.F. Awad, F.S. El-Shenawy, A.M.A. El-Bondkly, Production, purification, characterization, antioxidant and antiproliferative activities of extracellular L-asparaginase produced by *Fusarium equiseti* AHMF4, Saudi J. Biol. Sci. 28 (4) (2021) 2540–2548.

[60] M.L. Hutchings, C.J. Alpha-Cobb, D.A. Hiller, J. Berro, S.A. Strobel, Mycofumigation through production of the volatile DNA-methylating agent N-methyl-N-nitrosoisobutyramide by fungi in the genus *Muscodor*, Biol. Chem. 292 (18) (2017) 7358–7371, https://doi.org/10.1074/jbc.M117.779009J.

[61] A. Srivastava, A.K. Srivastava, A. Vishwkarma, O.P. Pandey, S.K. Sengupta, Synthesis, spectroscopic studies and biological aspects of bis(cyclopentadienyl) titanium(IV) complexes with 4-amino-5-(nicotinic/picolinic/isonicotinic/indole-3-propyl/indole-3-ethyl)-3-mercapto-1,2,4-triazole, J. Indian Chem. Soc. 97 (11b) (2020) 2363–2371.

[62] F. Tümer, M. Köse, M. Tümer, S.A. Güngör, S. Şahin, Absorption, redox and aggregation properties of new α,α-diamino-porphyrin based ligands and their Cu(II) complexes, J. Mol. Struct. 1190 (2019) 148–159.

[63] B. Godlewska-Żyłkiewicz, R. Świsłocka, M. Kalinowska, A. Golonko, G. Świderski, Ż. Arciszewska, E. Nalewajko-Sieliwoniuk, M. Naumowicz, W. Lewandowski, Biologically active compounds of plants: structure-related antioxidant, microbiological and cytotoxic activity of selected carboxylic acids, 8, Materials 13 (19) (2020) 4454, https://doi.org/10.3390/ma13194454. PMID: 33049979; PMCID: PMC7579235.

[64] E.R. El-Sayed, M.A. Hazaa, M.M. Shebl, M.M. Amer, S.R. Mahmoud, A.A. Khattab, Bioprospecting endophytic fungi for bioactive metabolites and use of irradiation to improve their bioactivities, Amb. Express 12 (1) (2022) 46, https://doi.org/10.1186/s13568-022-01386-x, 19.

[65] S. Caglar, A. Altay, M. Kuzucu, B. Caglar, In vitro anticancer activity of novel Co (II) and Ni (II) complexes of non-steroidal anti-inflammatory drug niflumic acid against human breast adenocarcinoma MCF-7 cells, Cell Biochem. Biophys. 79 (4) (2021) 729–746, https://doi.org/10.1007/s12013-021-00984-z.

[66] S. Perontsis, A.G. Hatzidimitriou, A.N. Papadopoulos, G.J. Psomas, Nickel-diflunisal complexes: synthesis, characterization, in vitro antioxidant activity and interaction with DNA and albumins, Inorg. Biochem. 162 (2016) 9–21, https://doi.org/10.1016/j.jinorgbio.2016.06.003.

[67] A. Tarushi, Z. Karaflou, J. Kljun, I. Turel, G. Psomas, A.N. Papadopoulos, D.P.J. Kessissoglou, Antioxidant capacity and DNA-interaction studies of zinc complexes with a non-steroidal anti-inflammatory drug, mefenamic acid, Inorg. Biochem. 128 (2013) 85–96, https://doi.org/10.1016/j.jinorgbio.2013.07.013.

[68] D.A.D.A. Aljuboury, P. Palaniandy, H.B. Abdul Aziz, S. Feroz, Treatment of petroleum wastewater by conventional and new technologies—a review, Glob. Nest J. 19 (2017) 439–452.

[69] K.T. Amakiri, A.R. Canon, M. Molinari, A. Angelis-Dimakis, Review of petroleum oilfield produced water treatment technologies, Chemosphere 298 (2022) 134064.

[70] M.M. Zareh, A.S. El-Sayed, D.M. El-Hady, Biosorption bioremoval of iron from water by *Aspergil*lus *Niger* NPJ, Clean. Water(Washingt.) 5 (1) (2022), https://doi.org/10.1038/s41545-022-00201-1.

[71] S.J. Alhamd, M.N. Abbas, M. Manteghian, T.A. Ibrahim, K.D.S. Jarmondi, Treatment of oil refinery wastewater polluted by heavy metal ions via bioremoval technique using non-valuable media: cadmium ions and buckthorn leaves as a study case, Karbala International Journal of Modern Science 10 (1) (2024), https://doi.org/10.33640/2405-609X.3334. Article 1.

[72] S. Ho, I. Cm, S. Cn, Bioremoval of heavy metals from effluent of port harcourt refinery using *pluer*otus o*streatus*, J. Petrol Environ. Biotechnol. 8 (2017) 1000324.